chapter**FOURTEEN**

Applications of Ultraviolet-Visible Molecular Absorption Spectrometry

Ultraviolet and visible absorption measurements are widely used for the identification and determination of many different inorganic and organic species. In fact, UV-visible molecular absorption methods are probably the most widely used of all quantitative analysis techniques in chemical, environmental, forensic, and clinical laboratories throughout the world.

Throughout this chapter, this logo indicates an opportunity for online self-study at **www.tinyurl.com/skoogpia7**, linking you to interactive tutorials, simulations, and exercises.

14A THE MAGNITUDE OF MOLAR ABSORPTIVITIES

Empirically, molar absorptivities (ε values) that range from zero to greater than 10^5 L mol^{-1} cm^{-1} are observed in ultraviolet (UV)-visible molecular absorption spectrometry.[1] For any particular absorption maximum, the magnitude of ε depends on the capture cross section (Section 13B, Equation 13-5) of the species and the probability for an energy-absorbing transition to occur. The relationship between ε and these variables has been shown to be

$$\varepsilon = 8.7 \times 10^{19} PA$$

where P is the transition probability and A is the cross-section target area in square centimeters per molecule.[2] The area for typical organic molecules has been estimated from electron diffraction and X-ray studies to be about 10^{-15} cm^2/molecule; transition probabilities vary from zero to one. For quantum mechanically allowed transitions, values of P range from 0.1 to 1, which leads to strong absorption bands ($\varepsilon_{max} = 10^4$ to 10^5 L mol^{-1} cm^{-1}). Absorption maxima having molar absorptivities less than about 10^3 are classified as being of low intensity. They usually result from forbidden transitions, which have probabilities of occurrence that are less than 0.01.

14B ABSORBING SPECIES

The absorption of UV or visible radiation by an atomic or molecular species M can be considered to be a two-step process. The first step involves electronic excitation as shown by the equation

$$M + h\nu \rightarrow M^*$$

[1]Some useful references on absorption methods include E. J. Meehan, in *Treatise on Analytical Chemistry*, 2nd ed., P. J. Elving, E. J. Meehan, and I. M. Kolthoff, eds., Part I, Vol. 7, Chaps. 1–3, New York: Wiley, 1981; R. P. Bauman, *Absorption Spectroscopy*, New York: Wiley, 1962; F. Grum, in *Physical Methods of Chemistry*, A. Weissberger and B. W. Rossiter, eds., Vol. I, Part III B, Chap. 3, New York: Wiley-Interscience, 1972; H. H. Jaffé and M. Orchin, *Theory and Applications of Ultraviolet Spectroscopy*, New York: Wiley, 1962; G. F. Lothian, *Absorption Spectrophotometry*, 3rd ed., London: Adam Hilger, 1969; J. D. Ingle Jr. and S. R. Crouch, *Spectrochemical Analysis*, Chap. 13, Upper Saddle River, NJ: Prentice-Hall, 1988.

[2]E. A. Braude, *J. Chem. Soc.*, **1950**, 379, **DOI**: 10.1039/jr9500000379.

The product of the absorption of the photon $h\nu$ by species M is an electronically excited species symbolized by M*. The lifetime of the excited species is brief (10^{-8} to 10^{-9} s). Any of several relaxation processes can lead to deexcitation of M*. The most common type of relaxation involves conversion of the excitation energy to heat as shown by

$$M^* \rightarrow M + \text{heat}$$

Relaxation may also occur by a photochemical process such as decomposition of M* to form new species. Alternatively, relaxation may involve reemission of a photon by fluorescence or phosphorescence. It is important to note that the lifetime of M* is usually so very short that its concentration at any instant is ordinarily negligible. Furthermore, the amount of thermal energy evolved by relaxation is quite small. Thus, absorption measurements create a minimal disturbance of the system under study except when photochemical decomposition occurs.

The absorption of UV or visible radiation generally results from excitation of bonding electrons. Because of this, the wavelengths of absorption bands can be correlated with the types of bonds in the species under study. Molecular absorption spectroscopy is, therefore, valuable for identifying functional groups in a molecule. More important, however, are the applications of UV and visible absorption spectroscopy to the quantitative determination of compounds containing absorbing groups.

As noted in Section 6C, absorption of UV and visible radiation by molecules generally occurs in one or more electronic absorption bands, each of which is made up of many closely packed but discrete lines. Each line arises from the transition of an electron from the ground state to one of the many vibrational and rotational energy states associated with each excited electronic energy state. Because there are so many of these vibrational and rotational states and because their energies differ only slightly, many closely spaced lines are contained in the typical band.

As can be seen in Figure 14-1a, the visible absorption spectrum for 1,2,4,5-tetrazine vapor shows the fine structure that is due to the numerous rotational and vibrational levels associated with the excited electronic states of this aromatic molecule. In the gaseous state, the individual tetrazine molecules are sufficiently separated from one another to vibrate and rotate freely, and the many individual absorption lines appear as a result of the large number of vibrational and rotational energy states. In the condensed state or in solution, however, the tetrazine molecules have little freedom to rotate, so lines due to differences in rotational energy levels disappear. Furthermore, when solvent molecules surround the tetrazine molecules, energies of the various vibrational levels are modified in a nonuniform way, and the energy of a given state in a sample of solute molecules appears as a single, broad peak. This effect is more pronounced in polar solvents, such as water, than in nonpolar hydrocarbon media. This solvent effect is illustrated in Figure 14-1b and c.

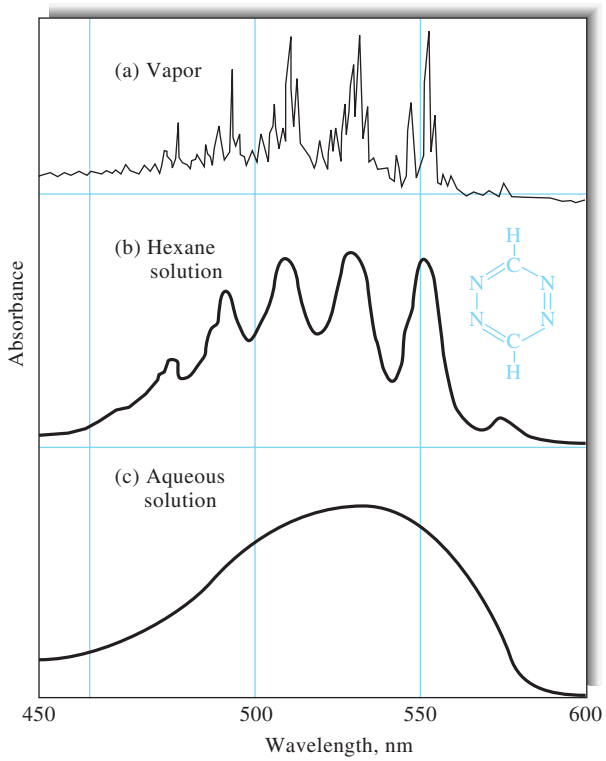

FIGURE 14-1 Ultraviolet absorption spectra for 1,2,4,5-tetrazine. In (a), the spectrum is shown in the gas phase, where many lines due to electronic, vibrational, and rotational transitions can be seen. In a nonpolar solvent (b), the electronic transitions can be observed, but the vibrational and rotational structure has been lost. In a polar solvent (c), the strong intermolecular forces cause the electronic peaks to blend, giving only a single smooth absorption band. (From S. F. Mason, *J. Chem. Soc.*, **1959**, 1265, **DOI**: 10.1039/jr9590001263.)

14B-1 Absorption by Organic Compounds

All organic compounds are capable of absorbing electromagnetic radiation because all contain valence electrons that can be excited to higher energy levels. The excitation energies associated with electrons forming most single bonds are sufficiently high that absorption occurs in the so-called vacuum UV region ($\lambda < 185$ nm), where components of the atmosphere also absorb radiation strongly. Such transitions involve the excitation of nonbonding n electrons to σ^* orbitals. The molar absorptivities of $n \rightarrow \sigma^*$ transitions are low to intermediate and usually range between 100 and 3000 L mol^{-1} cm^{-1}. Because of experimental difficulties associated with the vacuum UV region, most spectrophotometric investigations of organic compounds have involved longer wavelengths than 185 nm.

Most applications of absorption spectroscopy to organic compounds are based on transitions for n or π electrons to the π^* excited state because the energies required for these processes bring the absorption bands into the UV-visible region (200 to 700 nm). Both $n \rightarrow \pi^*$ and $\pi \rightarrow \pi^*$ transitions require the presence of an unsaturated functional group to provide the π orbitals. Molecules containing such functional groups and capable of absorbing UV-visible radiation are called *chromophores*.

TABLE 14-1 Absorption Characteristics of Some Common Chromophores

Chromophore	Example	Solvent	λ_{max}, nm	ε_{max}	Transition Type
Alkene	$C_6H_{13}CH{=}CH_2$	*n*-Heptane	177	13,000	$\pi \rightarrow \pi^*$
Alkyne	$C_5H_{11}CH{\equiv}C{-}CH_3$	*n*-Heptane	178	10,000	$\pi \rightarrow \pi^*$
			196	2000	—
			225	160	—
Carbonyl	$CH_3\overset{\overset{O}{\|}}{C}CH_3$	*n*-Hexane	186	1000	$n \rightarrow \sigma^*$
			280	16	$n \rightarrow \pi^*$
	$CH_3\overset{\overset{O}{\|}}{C}H$	*n*-Hexane	180	large	$n \rightarrow \sigma^*$
			293	12	$n \rightarrow \pi^*$
Carboxyl	CH_3COOH	Ethanol	204	41	$n \rightarrow \pi^*$
Amido	$CH_3\overset{\overset{O}{\|}}{C}NH_2$	Water	214	60	$n \rightarrow \pi^*$
Azo	$CH_3N{=}NCH_3$	Ethanol	339	5	$n \rightarrow \pi^*$
Nitro	CH_3NO_2	Isooctane	280	22	$n \rightarrow \pi^*$
Nitroso	C_4H_9NO	Ethyl ether	300	100	—
			665	20	$n \rightarrow \pi^*$
Nitrate	$C_2H_5ONO_2$	Dioxane	270	12	$n \rightarrow \pi^*$

The electronic spectra of organic molecules containing chromophores are usually complex, because the superposition of vibrational transitions on the electronic transitions leads to an intricate combination of overlapping lines. The result is a broad band of absorption that often appears to be continuous. The complex nature of the spectra makes detailed theoretical analysis difficult or impossible. Nevertheless, qualitative or semiquantitative statements concerning the types of electronic transitions responsible for a given absorption spectrum can be deduced from molecular orbital considerations.

Table 14-1 lists the common organic chromophores and the approximate wavelengths at which they absorb. The data for position (λ_{max}) and peak intensity (ε_{max}) can serve as only a rough guide for identification purposes, because both are influenced by solvent effects as well as other structural details of the molecule. In addition, conjugation between two or more chromophores tends to cause shifts in absorption maxima to longer wavelengths. Finally, vibrational effects broaden absorption peaks in the UV and visible regions, which often makes precise determination of an absorption maximum difficult. The molar absorptivities for $n \rightarrow \pi^*$ transitions are normally low and usually range from 10 to 100 L mol^{-1} cm^{-1}. On the other hand, values for $\pi \rightarrow \pi^*$ transitions generally range between 1000 and 15,000 L mol^{-1} cm^{-1}. Typical absorption spectra are shown in Figure 14-2.

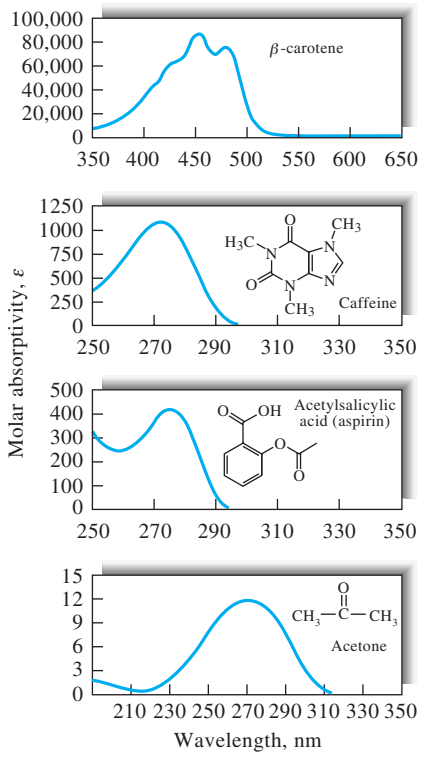

FIGURE 14-2 Absorption spectra for typical organic compounds.

TABLE 14-2 Absorption by Organic Compounds Containing Heteroatoms with Nonbonding Electrons

Compound	λ_{max}, nm	ε_{max}
CH_3OH	167	1480
$(CH_3)_2O$	184	2520
CH_3Cl	173	200
CH_3I	258	365
$(CH_3)_2S$	229	140
CH_3NH_2	215	600
$(CH_3)_3N$	227	900

Saturated organic compounds containing such heteroatoms as oxygen, nitrogen, sulfur, or halogens have nonbonding electrons that can be excited by radiation in the range of 170 to 250 nm. Table 14-2 lists a few examples of such compounds. Some of these compounds, such as alcohols and ethers, are common solvents, so their absorption in this region prevents measuring absorption of analytes dissolved in these compounds at wavelengths shorter than 180 to 200 nm. Occasionally, absorption in this region is used for determining halogen and sulfur-bearing compounds.

14B-2 Absorption by Inorganic Species

A number of inorganic anions exhibit UV absorption bands that are a result of exciting nonbonding electrons. Examples include nitrate (313 nm), carbonate (217 nm), nitrite (360 and 280 nm), azido (230 nm), and trithiocarbonate (500 nm) ions.

In general, the ions and complexes of elements in the first two transition series absorb broad bands of visible radiation in at least one of their oxidation states and are, as a result, colored (see, for example, Figure 14-3). Here, absorption involves transitions between filled and unfilled *d*-orbitals with energies that depend on the ligands bonded to the metal ions. The energy differences between these *d*-orbitals (and thus the position of the corresponding absorption maximum) depend on the position of the element in the periodic table, its oxidation state, and the nature of the ligand bonded to it.

Absorption spectra of ions of the lanthanide and actinide transitions series differ substantially from those shown in Figure 14-3. The electrons responsible for absorption by these elements (4*f* and 5*f*, respectively) are shielded from external influences by electrons that occupy orbitals with larger principal quantum numbers. As a result, the bands tend to be narrow and relatively unaffected by the species bonded by the outer electrons (see Figure 14-4).

14B-3 Charge-Transfer Absorption

For quantitative purposes, charge-transfer absorption is particularly important because molar absorptivities are unusually large ($\varepsilon > 10{,}000$ L mol^{-1} cm^{-1}), which leads to high sensitivity.

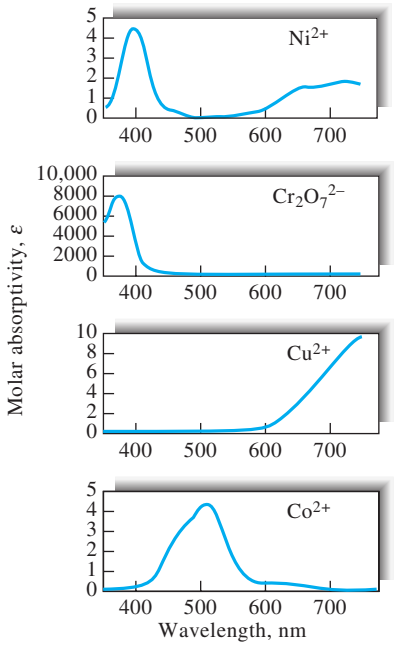

FIGURE 14-3 Absorption spectra of aqueous solutions of transition metal ions.

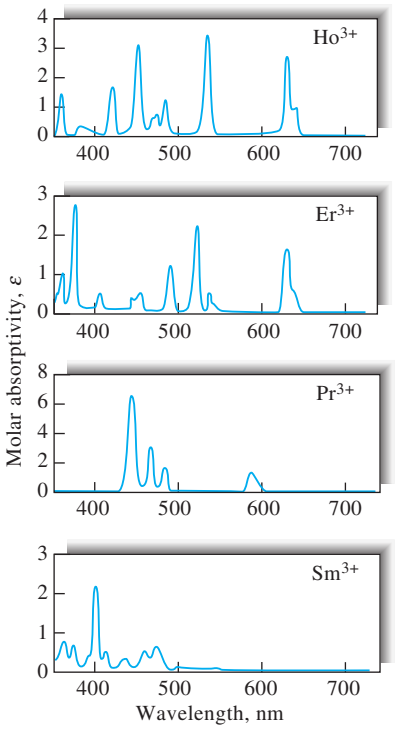

FIGURE 14-4 Absorption spectra of aqueous solutions of rare earth ions.

Many inorganic and organic complexes exhibit this type of absorption and are therefore called charge-transfer complexes.

A charge-transfer complex consists of an electron-donor group bonded to an electron acceptor. When this product absorbs radiation, an electron from the donor is transferred to

an orbital that is largely associated with the acceptor. The excited state is thus the product of a kind of internal oxidation-reduction process. This behavior differs from that of an organic chromophore in which the excited electron is in a molecular orbital shared by two or more atoms.

Familiar examples of charge-transfer complexes include the phenolic complex of iron(III), the 1,10-phenanthroline complex of iron(II), the iodide complex of molecular iodine, and the hexacyanoferrate(II)-hexacyanoferrate(III) complex responsible for the color of Prussian blue. The red color of the iron(III)-thiocyanate complex is a further example of charge-transfer absorption. Absorption of a photon results in the transfer of an electron from the thiocyanate ion to an orbital that is largely associated with the iron(III) ion. The product is an excited species involving predominantly iron(II) and the thiocyanate radical SCN. As with other types of electronic excitation, the electron in this complex ordinarily returns to its original state after a brief period. Occasionally, however, an excited complex may dissociate and produce photochemical oxidation-reduction products. Three spectra of charge-transfer complexes are shown in Figure 14-5.

In most charge-transfer complexes involving a metal ion, the metal serves as the electron acceptor. Exceptions are the 1,10-phenanthroline complexes of iron(II) and copper(I), where the ligand is the acceptor and the metal ion the donor. A few other examples of this type of complex are known.

Organic compounds form many interesting charge-transfer complexes. An example is quinhydrone (a 1:1 complex of quinone and hydroquinone), which exhibits strong absorption in the visible region. Other examples include iodine complexes with amines, aromatics, and sulfides.

Simulation: Learn more about **absorption spectra** at www.tinyurl.com/skoogpia7

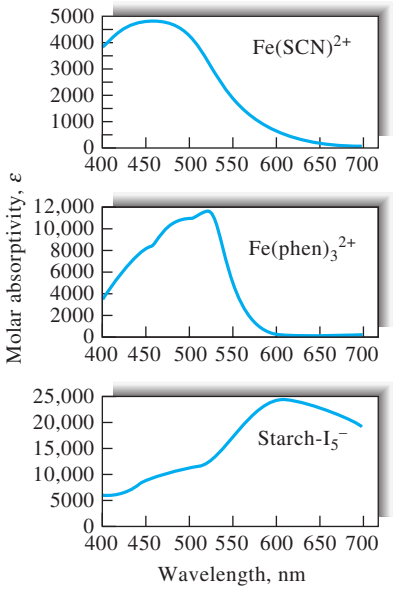

FIGURE 14-5 Absorption spectra of aqueous charge-transfer complexes.

14C QUALITATIVE APPLICATIONS OF ULTRAVIOLET VISIBLE ABSORPTION SPECTROSCOPY

Spectrophotometric measurements with UV radiation are useful for detecting chromophoric groups, such as those shown in Table 14-1.[3] Because large parts of even the most complex organic molecules are transparent to radiation longer than 180 nm, the appearance of one or more peaks in the region from 200 to 400 nm is clear indication of the presence of unsaturated groups or of atoms such as sulfur or halogens. Often, the identity of the absorbing groups can be determined by comparing the spectrum of an analyte with those of simple molecules containing various chromophoric groups.[4] Usually, however, UV spectra do not have enough fine structure to permit an analyte to be identified unambiguously. Thus, UV qualitative data must be supplemented with other physical or chemical evidence such as infrared, nuclear magnetic resonance, and mass spectra as well as solubility and melting- and boiling-point information.

14C-1 Solvents

UV spectra for qualitative analysis are usually measured using dilute solutions of the analyte. For volatile compounds, however, gas-phase spectra are often more useful than liquid-phase or solution spectra (for example, compare Figure 14-1a and b). Gas-phase spectra can often be obtained by allowing a drop or two of the pure liquid to evaporate and equilibrate with the atmosphere in a stoppered cuvette.

If a solvent is used, consideration must be given not only to its transparency, but also to its possible effects on the absorbing system. Quite generally, polar solvents such as water, alcohols, esters, and ketones tend to obliterate spectral fine structure arising from vibrational effects. Spectra similar to gas-phase spectra (see Figure 14-6) are more likely to be observed in nonpolar solvents such as hydrocarbons. In addition, the positions

[3]For a detailed discussion of UV absorption spectroscopy in the identification of organic functional groups, see R. M. Silverstein, G. C. Bassler, and T. C. Morrill, *Spectrometric Identification of Organic Compounds*, 5th ed., Chap. 6, New York: Wiley, 1991.

[4]H. H. Perkampus, *UV-VIS Atlas of Organic Compounds*, 2nd ed., Hoboken, NJ: Wiley-VCH, 1992. In addition, in the past, several organizations have published catalogs of spectra that may still be useful, including American Petroleum Institute, Ultraviolet Spectral Data, *A.P.I. Research Project 44*. Pittsburgh: Carnegie Institute of Technology; *Sadtler Handbook of Ultraviolet Spectra*, Philadelphia: Sadtler Research Laboratories; American Society for Testing Materials, Committee E-13, Philadelphia.

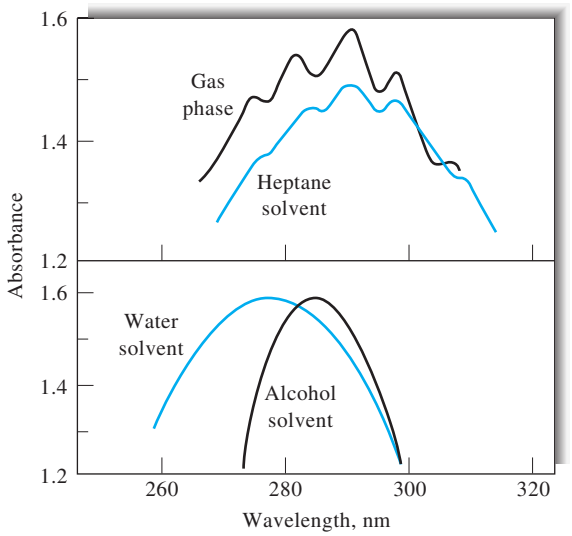

FIGURE 14-6 Effect of solvent on the absorption spectrum of acetaldehyde.

TABLE 14-3 Solvents for the UV and Visible Regions

Solvent	Lower Wavelength Limit, nm	Solvent	Lower Wavelength Limit, nm
Water	180	Diethyl ether	210
Ethanol	220	Acetone	330
Hexane	200	Dioxane	320
Cyclohexane	200	Cellosolve	320
Carbon tetrachloride	260		

of absorption maxima are influenced by the nature of the solvent. As a rule, the same solvent must be used when comparing absorption spectra for identification purposes.

Table 14-3 lists some common solvents and the approximate wavelength below which they cannot be used because of absorption. These wavelengths, called the *cutoff wavelengths*, depend strongly on the purity of the solvent.[5] Common solvents for UV spectrophotometry include water, 95% ethanol, cyclohexane, and 1,4-dioxane. For the visible region, any colorless solvent is suitable.

[5]Most major suppliers of reagent chemicals in the United States offer spectrochemical grades of solvents. Spectral-grade solvents have been treated to remove absorbing impurities and meet or exceed the requirements set forth in *Reagent Chemicals*, 10th ed., Washington, DC: American Chemical Society, 2005. *Reagent Chemicals* online is available at http://pubs.acs.org/reagents/index.html. Hardcover is available from the Oxford University Press website, http://www.oup.com/us/brochure/0841239452/?view=usa.

14C-2 The Effect of Slit Width

The effect of variation in slit width, and hence effective bandwidth, was shown previously for gas-phase spectra in Figure 13-8. The effect on solution spectra is illustrated for reduced cytochrome *c* in Figure 14-7. The plots show that peak heights and separation are distorted at wider bandwidths. Because of this, spectra for qualitative applications should be measured with minimum slit widths.

14C-3 Detection of Functional Groups

Even though it may not provide the unambiguous identification of an organic compound, an absorption spectrum in the visible and the UV regions is nevertheless useful for detecting the presence of certain functional groups that act as chromophores. For example, a weak absorption band in the region of 280 to 290 nm, which is displaced toward shorter wavelengths with increased solvent polarity, strongly indicates the presence of a carbonyl group. Such a shift is termed a *hypsochromic*, or *blue*, *shift*. A weak absorption band at about 260 nm with indications of vibrational fine structure constitutes evidence for the existence of an aromatic ring. Confirmation of the presence of an aromatic amine or a phenolic structure may be obtained by comparing the effects of pH on the spectra of solutions containing the sample with those shown in Table 14-4 for phenol and aniline.

The UV spectra of aromatic hydrocarbons are characterized by three sets of bands that originate from $\pi \rightarrow \pi^*$ transitions. For example, benzene has a strong absorption peak at 184 nm ($\varepsilon_{max} \approx 60{,}000$); a weaker band, called the E_2 band, at 204 nm ($\varepsilon_{max} = 7900$); and a still weaker peak, termed the B band, at 256 ($\varepsilon_{max} = 200$). The long-wavelength bands of benzene vapor, 1,2,4,5-tetrazine (see Figure 14-1a), and many other aromatics contain a series of sharp peaks due to the superposition of vibrational transitions on the basic electronic transitions. As shown in Figure 14-1, solvents tend to reduce (or sometimes eliminate) this fine structure as do certain types of substitution.

All three of the characteristic bands for benzene are strongly affected by ring substitution; the effects on the two

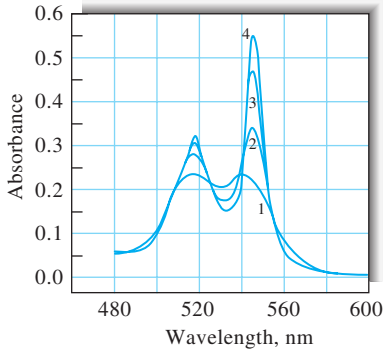

FIGURE 14-7 Spectra for reduced cytochrome *c* at four spectral bandwidths. (1) 20 nm, (2) 10 nm, (3) 5 nm, and (4) 1 nm. (Courtesy of Agilent Technologies, Inc., Santa Clara, CA.)

TABLE 14-4 Absorption Characteristics of Aromatic Compounds

Compound		E_2 Band		B Band	
		λ_{max}, nm	ε_{max}	λ_{max}, nm	ε_{max}
Benzene	C_6H_6	204	7900	256	200
Toluene	$C_6H_5CH_3$	207	7000	261	300
m-Xylene	$C_6H_4(CH_3)_2$	—	—	263	300
Chlorobenzene	C_6H_5Cl	210	7600	265	240
Phenol	C_6H_5OH	211	6200	270	1450
Phenolate ion	$C_6H_5O^-$	235	9400	287	2600
Aniline	$C_6H_5NH_2$	230	8600	280	1430
Anilinium ion	$C_6H_5NH_3^+$	203	7500	254	160
Thiophenol	C_6H_5SH	236	10,000	269	700
Naphthalene	$C_{10}H_8$	286	9300	312	289
Styrene	$C_6H_5CH{=}CH_2$	244	12,000	282	450

longer-wavelength bands are of particular interest because they can be studied with ordinary spectrophotometric equipment. Table 14-4 illustrates the effects of some common ring substituents.

By definition, an *auxochrome* is a functional group that does not itself absorb in the UV region but has the effect of shifting chromophore peaks to longer wavelengths as well as increasing their intensities. Such a shift to longer wavelengths is called a *bathochromic*, or *red*, *shift*. Note in Table 14-4 that —OH and $—NH_2$ have an auxochromic effect on the benzene chromophore, particularly with respect to the B band. Auxochromic substituents have at least one pair of *n* electrons capable of interacting with the π electrons of the ring. This interaction apparently has the effect of stabilizing the π^* state, thereby lowering its energy, and increasing the wavelength of the corresponding band. Note that the auxochromic effect is more pronounced for the phenolate anion than for phenol itself, probably because the anion has an extra pair of unshared electrons to contribute to the interaction. With aniline, on the other hand, the nonbonding electrons are lost by formation of the anilinium cation, and the auxochromic effect disappears.

14D QUANTITATIVE ANALYSIS BY ABSORPTION MEASUREMENTS

Absorption spectroscopy based on UV and visible radiation is one of the most useful tools available to the scientist for quantitative analysis.[6] Important characteristics of spectrophotometric and photometric methods include (1) wide applicability to both organic and inorganic systems, (2) typical detection limits of 10^{-4} to 10^{-5} M (in some cases, certain modifications can lead to lower limits of detection),[7] (3) moderate to high selectivity, (4) good accuracy (typically, relative uncertainties are 1% to 3%, although with special precautions, errors can be reduced to a few tenths of a percent), and (5) ease and convenience of data acquisition.

14D-1 Scope

The applications of quantitative, UV visible absorption methods not only are numerous but also touch on every field that requires quantitative chemical information. The reader can obtain a notion of the scope of spectrophotometry by consulting the series of review articles that were published in *Analytical Chemistry*[8] as well as monographs on the subject.[9]

Applications to Absorbing Species

Tables 14-1, 14-2, and 14-4 list many common organic chromophoric groups. Spectrophotometric determination of any organic compound containing one or more of these groups is potentially feasible. Many examples of this type of determination are found in the literature.

A number of inorganic species also absorb UV-visible radiation and are thus susceptible to direct determination.

[6]For a wealth of detailed, practical information on spectrophotometric practices, see *Techniques in Visible and Ultraviolet Spectrometry*, Vol. I, *Standards in Absorption Spectroscopy*, C. Burgess and A. Knowles, eds., London: Chapman & Hall, 1981; J. R. Edisbury, *Practical Hints on Absorption Spectrometry*, New York: Plenum Press, 1968.

[7]See, for example, T. D. Harris, *Anal. Chem.*, **1982**, *54*, 741A, **DOI**: 10.1021/ac00243a772.

[8]L. G. Hargis, J. A. Howell, and R. E. Sutton, *Anal. Chem.* (Review), **1996**, *68*, 169, **DOI**: 10.1021/a19600101; J. A. Howell and R. E. Sutton, *Anal. Chem.* (Review), **1998**, *70*, 107, **DOI**: 10.1021/a19800040.

[9]H. Onishi, *Photometric Determination of Traces of Metals*, Part IIA, Part IIB, 4th ed., New York: Wiley, 1986, 1989; *Colorimetric Determination of Nonmetals*, 2nd ed., D. F. Boltz, ed., New York: Interscience, 1978; E. B. Sandell and H. Onishi, *Photometric Determination of Traces of Metals*, 4th ed., New York: Wiley, 1978; F. D. Snell, *Photometric and Fluorometric Methods of Analysis*, New York: Wiley, 1978.

We have noted that many ions of the transition metals are colored in solution and can thus be determined by spectrophotometric measurement. In addition, a number of other species show characteristic absorption bands, including nitrite, nitrate, and chromate ions, the oxides of nitrogen, the elemental halogens, and ozone.

Applications to Nonabsorbing Species

Numerous reagents react selectively with nonabsorbing species to yield products that absorb strongly in the UV or visible regions. The successful application of such reagents to quantitative analysis usually requires that the color-forming reaction be forced to near completion. If the amount of product is limited by the analyte, the absorbance of the product is proportional to the analyte concentration. Kinetic methods are often based on the rate of formation of an absorbing product (see Section 14F). Color-forming reagents are frequently used as well for the determination of absorbing species, such as transition-metal ions. The molar absorptivity of the product is frequently orders of magnitude greater than that of the species before reaction.

A host of complexing agents are used to determine inorganic species. Typical inorganic reagents include thiocyanate ion for iron, cobalt, and molybdenum; hydrogen peroxide for titanium, vanadium, and chromium; and iodide ion for bismuth, palladium, and tellurium. Of even more importance are organic chelating agents that form stable, colored complexes with cations. Common examples include diethyldithiocarbamate for the determination of copper, diphenylthiocarbazone for lead, 1,10-phenanthrolene for iron, and dimethylglyoxime for nickel. In the application of the last reaction to the photometric determination of nickel, an aqueous solution of the cation is extracted with a solution of the chelating agent in an immiscible organic liquid. The absorbance of the resulting bright red organic layer serves as a measure of the concentration of the metal.

14D-2 Procedural Details

A first step in any photometric or spectrophotometric analysis is the development of conditions that yield a reproducible relationship (preferably linear) between absorbance and analyte concentration.

Selection of Wavelength

For highest sensitivity, spectrophotometric absorbance measurements are ordinarily made at a wavelength corresponding to an absorption maximum because the change in absorbance per unit of concentration is greatest at this point. In addition, the absorbance is nearly constant with wavelength at an absorption maximum, which minimizes deviations from Beer's law due to polychromatic radiation (see Figure 13-5). Finally, small uncertainties that arise from failing to reproduce precisely the wavelength setting of the instrument have less influence at an absorption maximum.

Variables That Influence Absorbance

Common variables that influence the absorption spectrum of a substance include the nature of the solvent, the pH of the solution, the temperature, high electrolyte concentrations, and the presence of interfering substances. The effects of these variables must be known and conditions for the analysis must be chosen such that the absorbance will not be materially influenced by small, uncontrolled variations in their magnitudes.

Cleaning and Handling of Cells

Accurate spectrophotometric analysis requires the use of good-quality, matched cells. These should be regularly calibrated against one another to detect differences that can result from scratches, etching, and wear. It is equally important to use proper cell-cleaning and drying techniques. Erickson and Surles[10] recommend the following cleaning sequence for the outside windows of cells. Prior to measurement, the cell surfaces should be cleaned with a lens paper soaked in spectrograde methanol. While wiping, it is best to wear gloves or to hold the paper with a hemostat. The methanol is then allowed to evaporate, leaving the cell surfaces free of contaminants. Erickson and Surles showed that this method was superior to the usual procedure of wiping the cell surfaces with a dry lens paper, which can leave lint and a film on the surface.

Determining the Relationship between Absorbance and Concentration

The method of external standards (see Section 1D-2) is most often used to establish the absorbance versus concentration relationship. After deciding on the conditions for the analysis, the calibration curve is prepared from a series of standard solutions that bracket the concentration range expected for the samples. Seldom, if ever, is it safe to assume adherence to Beer's law and use only a single standard to determine the molar absorptivity. Because molar absorptivities are dependent on many environmental factors, determinations should never be based on a literature value of absorptivity.

Ideally, calibration standards should approximate the composition of the samples to be analyzed not only with respect to the analyte concentration but also with regard to the concentrations of the other species in the sample matrix. This can minimize the effects of various components of the sample on the measured absorbance. For example, the absorbance of many colored complexes of metal ions is decreased to a varying degree in the presence of sulfate and phosphate ions because these anions can form colorless complexes with metal ions. The desired reaction is often less complete as a consequence, and lowered absorbances are the result. The matrix effect of sulfate and phosphate can often be counteracted by introducing into the standards amounts of the two species that approximate the amounts found in the samples. Unfortunately, matrix matching is often impossible or quite difficult when complex materials such as soils, minerals, and tissues are being analyzed. When this is the case, the *standard-addition method* is often helpful in counteracting matrix effects that affect the slope of the calibration curve. However, the standard-addition method does not compensate

[10] J. O. Erickson and T. Surles, *Amer. Lab.*, **1976**, *8* (6), 50.

for extraneous absorbing species unless they are present at the same concentration in the blank solution.

The Standard-Addition Method

The standard-addition method can take several forms.[11] The one most often chosen for photometric or spectrophotometric analyses, and the one that was discussed in some detail in Section 1D-3, involves adding one or more increments of a standard solution to sample aliquots. Each solution is then diluted to a fixed volume before measuring its absorbance. Example 14-1 illustrates a spreadsheet approach to the multiple-additions method for the photometric determination of nitrite.

EXAMPLE 14-1

Nitrite is commonly determined by a spectrophotometric procedure using the Griess reaction. The sample containing nitrite is reacted with sulfanilimide and N-(1-naphthyl)ethylenediamine to form a colored species that absorbs radiation at 550 nm. Five-milliliter aliquots of the sample were pipetted into five 50.00-mL volumetric flasks. Then, 0.00, 2.00, 4.00, 6.00, and 8.00 mL of a standard solution containing 10.00 μM nitrite were pipetted into each flask, and the color-forming reagents added. After dilution to volume, the absorbance for each of the five solutions was measured at 550 nm. The absorbances were 0.139, 0.299, 0.486, 0.689, and 0.865, respectively. Devise a spreadsheet to calculate the nitrite concentration in the original sample and its standard deviation.

Solution

The spreadsheet is shown in Figure 14-8. Note that the final result indicates the concentration of nitrite in the original sample is 2.8 ± 0.3 μM. The standard deviation is found from the regression line[12] by using an extrapolated x value of −1.385 mL and a y value of 0.000 as illustrated in Example 1-1 of Chapter 1.

In the interest of saving time or sample, it is possible to perform a standard-addition analysis using only two increments of sample. Here, a single addition of V_s mL of standard would be added to one of the two samples. This approach is based on Equation 14-1 (see Section 1D-3).

$$c_x = \frac{A_1 c_s V_s}{(A_2 - A_1)V_x} \qquad (14\text{-}1)$$

The single-addition method is illustrated in Example 14-2.

[11]See M. Bader, *J. Chem. Educ.*, **1980**, *57*, 703, **DOI**: 10.1021/ed057p703.

[12]For more information on spreadsheet approaches to standard addition methods, see S. R. Crouch and F. J. Holler, *Applications of Microsoft® Excel in Analytical Chemistry*, 3rd ed., Chaps. 4 and 12, Belmont, CA: Cengage Learning, 2017.

EXAMPLE 14-2

A 2.00-mL urine specimen was treated with reagent to generate a color with phosphate, following which the sample was diluted to 100 mL. To a second 2.00-mL sample was added exactly 5.00 mL of a phosphate solution containing 0.0300 mg phosphate/mL, which was treated in the same way as the original sample. The absorbance of the first solution was 0.428, and that of the second was 0.538. Calculate the concentration of phosphate in milligrams per millimeter of the specimen.

Solution

Here we substitute into Equation 14-1 and obtain

$$c_x = \frac{(0.428)(0.0300 \text{ mg } PO_4^{3-}/\text{mL})(5.00 \text{ mL})}{(0.538 - 0.428)(2.00 \text{ mL sample})}$$

$$= 0.292 \text{ mg } PO_4^{3-}/\text{mL sample}$$

Analysis of Mixtures of Absorbing Substances

The total absorbance of a solution at any given wavelength is equal to the sum of the absorbances of the individual components in the solution (Equation 13-9). This relationship makes it possible in principle to determine the concentrations of the individual components of a mixture even if their spectra overlap completely. For example, Figure 14-9 shows the spectrum of a solution containing a mixture of species M and species N as well as absorption spectra for the individual components. It is apparent that there is no wavelength where the absorbance is due to just one of these components. To analyze the mixture, molar absorptivities for M and N are first determined at wavelengths λ_1 and λ_2 with sufficient concentrations of the two standard solutions to be sure that Beer's law is obeyed over an absorbance range that encompasses the absorbance of the sample. Note that the wavelengths selected are ones at which the molar absorptivities of the two components differ significantly. Thus, at λ_1, the molar absorptivity of component M is much larger than that for component N. The reverse is true for λ_2. To complete the analysis, the absorbance of the mixture is determined at the same two wavelengths. From the known molar absorptivities and path length, the following equations hold:

$$A_1 = \varepsilon_{M_1} b c_M + \varepsilon_{N_1} b c_N \qquad (14\text{-}2)$$

$$A_2 = \varepsilon_{M_2} b c_M + \varepsilon_{N_2} b c_N \qquad (14\text{-}3)$$

where the subscript 1 indicates measurement at wavelength λ_1, and the subscript 2 indicates measurement at wavelength λ_2. With the known values of ε and b, Equations 14-2 and 14-3 represent two equations in two unknowns (c_M and c_N) that can be solved. The relationships are valid only if Beer's law holds at both wavelengths and the two components behave independently of one another. The greatest accuracy is obtained by choosing wavelengths at which the differences in molar absorptivities are large.

	A	B	C	D	E	F	G	H	I	J	K
1	**Determination of Nitrite in Water by Absorption Spectrophotometry**										
2	Concentration of standard, c_s	10.00	μM								
3	Volume of unknown used, V_x	5.00	mL								
4	**Volume of standard added**	***A***									
5	0.00	0.139									
6	2.00	0.299									
7	4.00	0.488									
8	6.00	0.689									
9	8.00	0.865									
10	**Regression Equation**										
11	Slope	0.0921									
12	Intercept	0.1276									
13	Volume intercept	-1.38545									
14	Concentration of unknown	2.7709									
15	**Error Analysis**										
16	Standard error in *y*	0.01205									
17	*N*	5									
18	S_{xx}	40.00									
19	*y* bar	0.4960									
20	Standard deviation in volume	0.1258									
21	Standard deviation in *c*	0.2517									
22	**Spreadsheet Documentation**										
23	Cell B11=SLOPE(B5:B9,A5:A9)										
24	Cell B12=INTERCEPT(B5:B9,A5:A9)										
25	Cell B13=-B12/B11										
26	Cell B14=-B13*B2/B3										
27	Cell B16=STEYX(B5:B9,A5:A9)										
28	Cell B17=COUNT(B5:B9)										
29	Cell B18=DEVSQ(A5:A9)										
30	Cell B19=AVERAGE(B5:B9)										
31	Cell B20=(B16/B11)*SQRT(1/B17+((0-B19)^2)/((B11^2)*B18))										
32	Cell B21=B20*B2/B3										

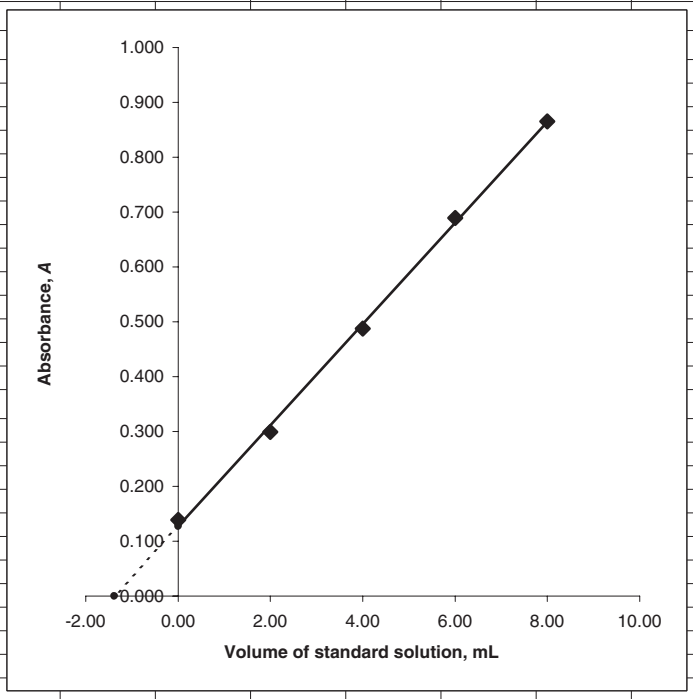

FIGURE 14-8 Spreadsheet to determine concentration of nitrite by multiple standard additions.

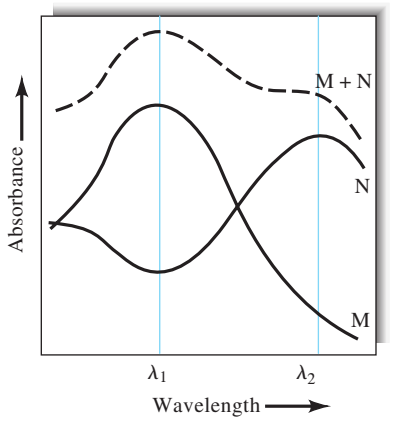

FIGURE 14-9 Absorption spectrum of a two-component mixture (M + N) with spectra of the individual components. Vertical dashed lines indicate optimal wavelengths for determination of the two components.

Mixtures containing more than two absorbing species can be analyzed, in principle at least, if a further absorbance measurement is made for each added component. The uncertainties in the resulting data become greater, however, as the number of measurements increases. Some array-detector spectrophotometers are capable of reducing these uncertainties by overdetermining the system. That is, these instruments use many more data points than unknowns and effectively match the entire spectrum of the unknown as closely as possible by least-squares techniques using the methods of matrix algebra. The spectra for standard solutions of each component are required for the analysis.

Computer data-processing methods based on factor analysis or principal components analysis have been developed to determine the number of components and their concentrations or absorptivities in mixtures.[13] These methods are usually applied to data obtained from array-detector-based spectrometers.

Tutorial: Learn more about **calibration and analysis of mixtures** at www.tinyurl.com/skoogpia7

14D-3 Derivative and Dual-Wavelength Spectrophotometry

In derivative spectrophotometry, spectra are obtained by plotting the first- or a higher-order derivative of absorbance with respect to wavelength as a function of wavelength.[14]

[13]E. R. Malinowski, *Factor Analysis in Chemistry*, 3rd ed., Chap. 9, New York: Wiley, 2002.

[14]For additional information see G. Talsky, *Derivative Spectrophotometry Low and High Order*, New York: VCH, 1994; T. C. O'Haver, *Anal. Chem.*, **1979**, *51*, 91A, **DOI**: 10.1021/ac50037a782; F. Sanchez Rojas, C. Bosch Ojeda, and J. M. Cano Pavon, *Talanta*, **1988**, *35*, 753, **DOI**: 10.1016/0039-9140(88)80179-6. For more recent reviews see, F. Sanchez Rojas and C. Bosch Ojeda, *Anal. Chim. Acta*, **2009**, *635*, 22, **DOI**: 10.1016/j.aca.2008.12.039; C. Bosch Ojeda and F. Sanchez Rojas, *Microchim. J.*, **2013**, *106*, 1, **DOI**: 10.1016/j.microc.2012.05.012.

Often, these plots reveal spectral detail that is lost in an ordinary spectrum. In addition, concentration measurements of an analyte in the presence of an interference or of two or more analytes in a mixture can sometimes be made more easily or more accurately using derivative methods. Unfortunately, the advantages of derivative spectra are at least partially offset by the degradation in signal-to-noise ratio that accompanies obtaining derivatives. In some parts of the UV and visible regions, however, signal-to-noise ratio is not a limiting factor. Even if signal-to-noise ratio is degraded by differentiation, smoothing methods can be applied to help improve precision.

Several different methods have been used to obtain derivative spectra. For modern computer-controlled digital spectrophotometers, the differentiation can be performed numerically using procedures such as derivative least-squares polynomial smoothing, which is discussed in Section 5C-2. With older analog instruments, derivatives of spectral data could be obtained electronically with a suitable operational amplifier circuit (see Section 3E-4). Another technique uses mechanical oscillation of a refractor plate to sweep a wavelength interval of a few nanometers repetitively across the exit slit of a monochromator while the spectrum is scanned, a technique known as *wavelength modulation*. Alternatively, the spectrum can be scanned using two wavelengths offset by a few nanometers, which is called *dual-wavelength spectrophotometry*.

Applications of Derivative Spectra

Many of the most important applications of derivative spectroscopy in the UV and visible regions have been for qualitative identification of species. The enhanced detail of a derivative spectrum makes it possible to distinguish among compounds having overlapping spectra, a technique often called *feature enhancement*.[15] Figure 14-10 illustrates how a derivative plot can reveal details of a spectrum consisting of three overlapping absorption peaks. It should be noted that taking a derivative enhances noise, and so high-quality spectra are essential for using this technique. If high-quality spectra are not used, derivative spectra can sometimes create features that are not actually present.

Derivative spectrophotometry is also proving quite useful for the simultaneous determination of two or more components in mixtures. With mixtures, several methods have been proposed for quantitative analysis. The peak-to-peak height has been used as has the peak height at the zero crossing wavelengths for the individual components. More recently, multivariate statistical techniques, such as partial least squares and principal components analysis, have been used to determine concentrations. Derivative methods have been used to determine trace metals in mixtures. For example, trace amounts of Mn and Zn can be determined in mixtures by forming complexes with 5,8-dihydroxy-1,4-naphthoquinone.[16] Derivative methods have also been widely applied to pharmaceutical preparations and to vitamin mixtures.[17]

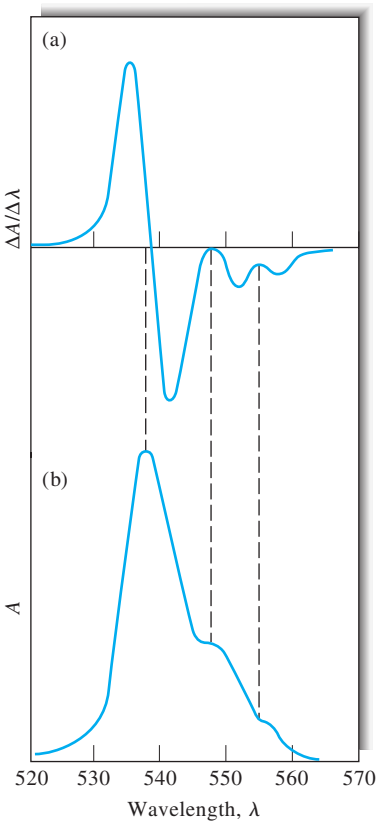

FIGURE 14-10 Comparison of a derivative spectrum (a) with a standard absorption spectrum (b).

Derivative and dual-wavelength spectrophotometry have also proved particularly useful for extracting UV visible absorption spectra of analytes present in turbid solutions, where light scattering obliterates the details of an absorption spectrum. For example, three amino acids, tryptophan, tyrosine, and phenylalanine, contain aromatic side chains, which exhibit sharp absorption bands in the 240 to 300-nm region. These sharp peaks are not, however, apparent in spectra of typical protein preparations, such as bovine or egg albumin, because the large protein molecules scatter radiation severely, yielding only a smooth absorption band such as that shown in Figure 14-11a. As shown in curves (b) and (c), the aromatic fine structure is revealed in first- and second-derivative spectra.

Dual-wavelength spectrophotometry has also proved useful for determination of an analyte in the presence of a spectral interference. Here, the instrument is operated in the

[15]Spreadsheet applications involving derivative techniques for feature enhancement are given in S. R. Crouch and F. J. Holler, *Applications of Microsoft® Excel in Analytical Chemistry*, 3rd ed., pp. 437–441, Belmont, CA: Cengage Learning, 2017.

[16]H. Sedaira, *Talanta*, **2000**, *51*, 39, **DOI**: 10.1016/S0039-9140(99)00244-1.

[17]F. Aberastuuri, A. I. Jimenez, F. Jimenez, and J. J. Arias, *J. Chem. Educ.*, **2001**, *78*, 793, **DOI**: 10.1021/ed078p793.

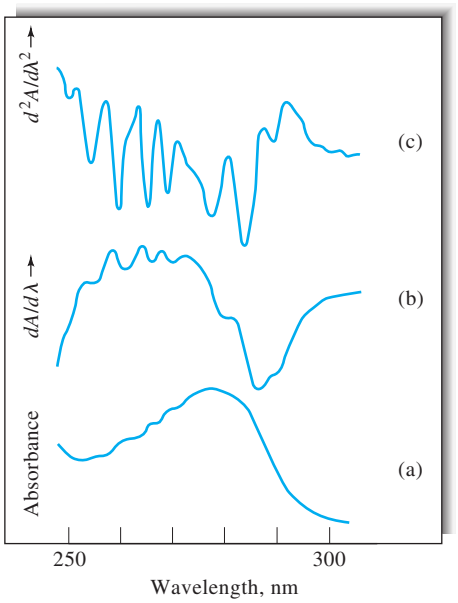

FIGURE 14-11 Absorption spectra of bovine albumin: (a) ordinary spectrum, (b) first-derivative spectrum, (c) second-derivative spectrum. (Reprinted with permission from J. E. Cahill and F. G. Padera, *Amer. Lab.*, **1980**, *12* (4), 109. Copyright 1980 by International Scientific Communications, Inc.)

nonscanning mode with absorbances being measured at two wavelengths at which the interference has identical molar absorptivities. In contrast, the analyte must absorb radiation more strongly at one of these wavelengths than the other. The differential absorbance is then directly proportional to the analyte concentration.

14E PHOTOMETRIC AND SPECTROPHOTOMETRIC TITRATIONS

Photometric or spectrophotometric measurements are useful for locating the equivalence point of a titration, provided the analyte, the reagent, or the titration product absorbs radiation.[18] Alternatively, an absorbing indicator can provide the absorbance change necessary for location of the equivalence point.

14E-1 Titration Curves

A photometric titration curve is a plot of absorbance, corrected for volume changes, as a function of the volume of titrant. For many titrations, the curve consists of two linear regions with differing slopes, one occurring early in the titration and the other located well beyond the equivalence-point region. The end point is the intersection of the extrapolated linear portions of the curve. End points can also be determined automatically by titration to a fixed absorbance or by taking the derivative to convert the linear-segment curve to a sigmoid-shape curve.

Figure 14-12 shows typical photometric titration curves. Figure 14-12a is the curve for the titration of a nonabsorbing species with an absorbing titrant that reacts with the analyte to form a nonabsorbing product. An example is the titration of thiosulfate ion with triiodide ion. The titration curve for the formation of an absorbing product from nonabsorbing reactants is shown in Figure 14-12b; an example is the titration of iodide ion with a standard solution of iodate ion to form triiodide. The remaining figures illustrate the curves obtained with various combinations of absorbing analytes, titrants, and products.

To obtain titration curves with linear portions that can be extrapolated, the absorbing systems must obey Beer's law. In addition, absorbances must be corrected for volume changes by multiplying the observed absorbance by $(V + v)/V$, where V is the original volume of the solution and v is the volume of added titrant. Many methods, however, use only changes in absorbance to locate the endpoints by various techniques. With these, strict adherence to Beer's law is not a necessity.

14E-2 Instrumentation

Photometric titrations are ordinarily performed with a spectrophotometer or a photometer that has been modified so that the titration vessel is held stationary in the light path. Alternatively, a probe-type cell, such as that shown in Figure 13-18, can be used. After the instrument is set to a suitable wavelength or an appropriate filter is inserted, the 0%T

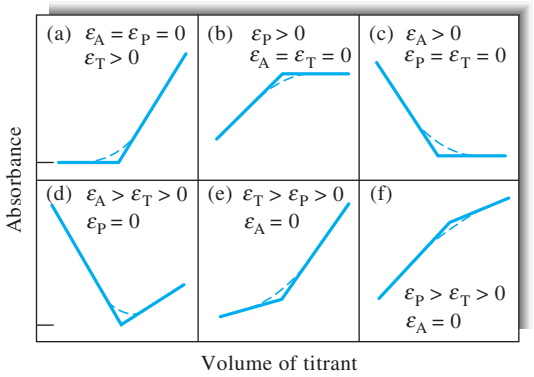

FIGURE 14-12 Typical photometric titration curves. Molar absorptivities of the analyte, the product, and the titrant are given by ε_A, ε_P, ε_T, respectively. The dashed lines represent actual data, and the solid lines are extrapolated from the linear portions of the plots.

[18]For further information concerning this technique, see J. B. Headridge, *Photometric Titrations*, New York: Pergamon, 1961; M. A. Leonard, in *Comprehensive Analytical Chemistry*, G. Svehla, ed., Vol. 8, Chap. 3, New York: Elsevier, 1977.

adjustment is made in the usual way. With radiation passing through the analyte solution to the transducer, the instrument is then adjusted to a convenient absorbance reading by varying the source intensity or the transducer sensitivity. It is not usually necessary to measure the true absorbance because relative values are perfectly adequate for end-point detection. Titration data are then collected without changing the instrument settings. The power of the radiation source and the response of the transducer must remain constant during a photometric titration. Cylindrical containers are often used in photometric titrations, and it is important to avoid moving the cell, so that the path length remains constant.

Both filter photometers and spectrophotometers have been used for photometric titrations. Several instrument companies currently produce photometric titration equipment.

14E-3 Applications of Photometric Titrations

Photometric titrations often provide more accurate results than a direct photometric analysis because the data from several measurements are used to determine the end point. Furthermore, the presence of other absorbing species may not interfere, because only a change in absorbance is being measured.

An advantage of end points determined from linear-segment photometric titration curves is that the experimental data are collected well away from the equivalence-point region where the absorbance changes gradually. In such cases, the equilibrium constant for the reaction need not be as large as that required for a sigmoid titration curve, which depends heavily on observations near the equivalence point (for example, potentiometric or indicator end points). For the same reason, more dilute solutions may be titrated using photometric detection.

The photometric end point has been applied to many types of reactions. For example, most standard oxidizing agents have characteristic absorption spectra and thus produce photometrically detectable end points. Although standard acids or bases do not absorb, the introduction of acid-base indicators permits photometric neutralization titrations. The photometric end point has also been used to great advantage in titrations with EDTA (ethylenediaminetetraacetic acid) and other complexing agents.[19] Figure 14-13a illustrates the application of this technique to the determination of total hardness in tap water using Eriochrome Black T as the indicator. The absorbance of the indicator is monitored at 610 nm.[20]

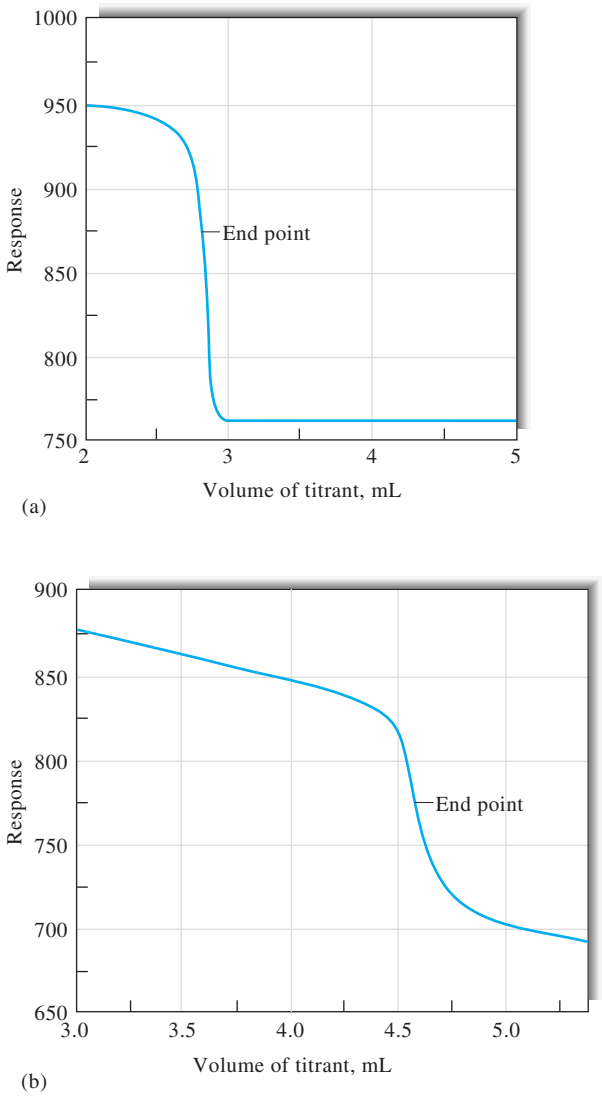

FIGURE 14-13 Photometric titration curves: (a) total hardness of water, (b) determination of sulfate. In (a), total water hardness is obtained by titration with 0.10 M EDTA at 610 nm for 100 mL of a solution that contained 2.82 mmol/L total hardness. Eriochrome Black T was the indicator. In (b), 10.0 mL of a solution containing sulfate was titrated with 0.050 M $BaCl_2$ using Thorin as an indicator and a wavelength of 523 nm. The response shown is proportional to transmittance. (From A. L. Underwood, *Anal. Chem.*, **1954**, *26*, 1322. Figure 1, p. 1323. Copyright 1954 American Chemical Society.)

The photometric end point has also been adapted to precipitation titrations. In *turbidimetric titrations*, the suspended solid product causes a decrease in the radiant power of the light source by scattering from the particles of the precipitate. The end point is observed when the precipitate stops forming and the amount of light reaching the detector becomes constant. The

Simulation: Learn more about **spectrophotometric titrations** at www.tinyurl.com/skoogpia7

[19]For a discussion of EDTA titrations, see D. A. Skoog, D. M. West, F. J. Holler, and S. R. Crouch, *Fundamentals of Analytical Chemistry*, 9th ed., Belmont, CA: Brooks/Cole, 2014, Chap. 17.

[20]For information on this method, see Metrohm, Application Note, 084, Metrohm USA, Riverview, FL.

end point in some precipitation titrations can also be detected as shown in Figure 14-13b by addition of an indicator. Here, the Ba^{2+} titrant reacts with SO_4^{2-} to form insoluble $BaSO_4$. Once the end point has been reached, the excess Ba^{2+} ions react with an indicator, Thorin, to form a colored complex that absorbs light at 523 nm.[21]

14F SPECTROPHOTOMETRIC KINETIC METHODS

Kinetic methods of analysis[22] differ in a fundamental way from the equilibrium, or stoichiometric, methods we have been considering. In kinetic methods, measurements are made under *dynamic* conditions in which the concentrations of reactants and products are changing as a function of time. In contrast, titrations or procedures using complexing agents to form absorbing products are performed on systems that have come to equilibrium or steady state so that concentrations are *static*. The majority of kinetic methods use spectrophotometry as the reaction monitoring technique.

The distinction between the two types of methods is illustrated in Figure 14-14, which shows the progress over time of the reaction

$$A + R \rightleftharpoons P \qquad (14\text{-}4)$$

where A represents the analyte, R the reagent, and P the product. Equilibrium methods operate in the region beyond time t_e, when the bulk concentrations of reactants and product have become constant and the chemical system is at equilibrium. In contrast, kinetic methods are carried out during the time interval from 0 to t_e, when analyte and product concentrations are changing continuously.

Kinetic methods can be more selective than equilibrium methods if reagents and conditions are chosen to maximize differences in the rates at which the analyte and potential interferents react. In equilibrium-based methods, selectivity is realized by maximizing differences in equilibrium constants.

14F-1 Types of Reactions

Kinetic methods can use several different types of reactions. Catalyzed reactions are among the most popular. With these, a catalyst is determined by its influence on the reaction rate or one of the reactants is determined. For example, iodide is a catalyst in the reaction of Ce(IV) with As(III). Trace quantities of I^- can be determined by measuring the rate of this reaction as a function of the I^- concentration. Normally, the method of external standards is used to prepare a calibration curve of rate versus iodide concentration. More than forty inorganic cations and more than fifteen anions have been determined based on their catalytic effect.

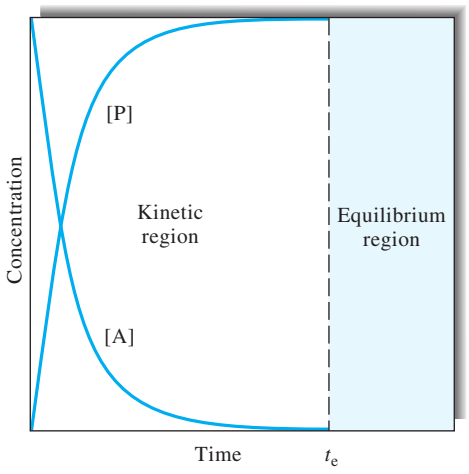

FIGURE 14-14 Change in concentration of analyte [A] and product [P] as a function of time. Until time t_e the analyte and product concentrations are continuously changing. This is the kinetic regime. In the equilibrium region, after t_e, the analyte and product concentrations are static.

Organic catalysts have also been determined by kinetic methods. The most important applications of catalyzed reactions to organic analyses involve the use of enzymes as catalysts. The behavior of a large number of enzymes is consistent with the general mechanism

$$E + S \underset{k_{-1}}{\overset{k_1}{\rightleftharpoons}} ES \xrightarrow{k_2} P + E \qquad (14\text{-}5)$$

In this so-called *Michaelis-Menten mechanism*, the enzyme E reacts reversibly with the substrate S to form an enzyme-substrate complex ES. This complex then decomposes irreversibly to form the products and the regenerated enzyme. The rate of this reaction often follows the rate law

$$\frac{d[P]}{dt} = \frac{k_2[E]_0[S]}{\dfrac{k_{-1} + k_2}{k_1} + [S]} = \frac{k_2[E]_0[S]}{K_m + [S]} \qquad (14\text{-}6)$$

where K_m is the Michaelis constant $(k_{-1} + k_2)/k_1$. Under conditions where the enzyme is saturated with substrate, $[S] \gg K_m$,

Simulation: Learn more about **kinetic methods** at www.tinyurl.com/skoogpia7

[21]See Metrohm, Application Bulletin, 140 Metrohm USA, Riverview, FL.

[22]For additional information, see D. A. Skoog, D. M. West, F. J. Holler, and S. R. Crouch, *Fundamentals of Analytical Chemistry*, 9th ed., Chap. 30, Belmont, CA: Brooks/Cole, 2014; H. O. Mottola, *Kinetic Aspects of Analytical Chemistry*, New York: Wiley, 1988.

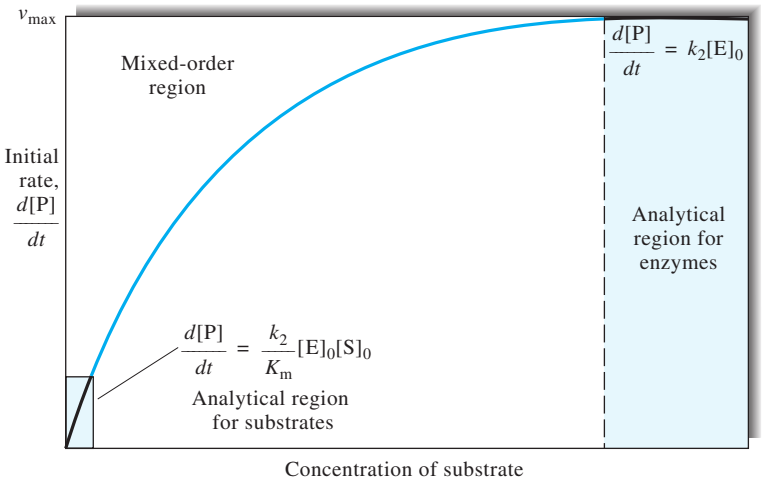

FIGURE 14-15 Plot of initial rate of product formation as a function of substrate concentration, showing the parts of the curve useful for the determination of substrate and enzyme.

the rate $d[P]/dt$ is directly proportional to the initial enzyme concentration $[E]_0$:

$$\frac{d[P]}{dt} = k_2[E]_0$$

Hence, measurements of the rate can be used to obtain the enzyme activity (concentration), $[E]_0$.

Substrates can also be determined by kinetic methods. Under conditions where $[S] \ll K_m$, Equation 14-6 reduces to

$$\frac{d[P]}{dt} = \frac{k_2}{K_m}[E]_0[S] = k'[S]$$

where $k' = k_2/K_m$. Here, the reaction rate is directly proportional to the substrate concentration, [S]. If measurements are made near the beginning of the reaction (<5% reaction), $[S] \approx [S]_0$ and the rate is directly proportional to the initial substrate concentration.[23]

The regions where enzyme and substrate can be determined by kinetic methods are illustrated in Figure 14-15, which shows a plot of initial rate versus substrate concentration. We can see that the initial rate is proportional to substrate concentration at very low concentrations, but the rate is proportional to the enzyme concentration when the substrate concentration is very high.

In addition to catalyzed reactions, kinetic methods of analysis also can use uncatalyzed reactions. As an example, phosphate can be determined by measuring the rate of its reaction with molybdate to form a heteropoly species, 12-molybdophosphate. More sensitivity can be achieved by reducing the 12-molybdophosphate with ascorbic acid or another reducing agent to form phosphomolybdenum blue, an intensely colored species. In either case, the rate of formation of the product is directly proportional to the phosphate concentration.

14F-2 Instrumentation

Kinetic methods based on reactions that, with half-lives greater than about 10 s, can be performed in an ordinary spectrophotometer equipped with a thermostatted cell compartment and provision to introduce and mix samples and reagents. Rates of reaction are highly dependent on temperature, and so temperature control to about 0.1°C is necessary for good reproducibility. Many commercial spectrophotometers have attachments that allow rates to be obtained. For very slow reactions, sample introduction and mixing can be accomplished prior to placing the reaction mixture in the cell compartment. Usually, however, a stationary cell is used, and all reagents except one are placed in the cell. The reagent needed to start the reaction is then introduced by syringe or pipette and the ensuing reaction is monitored while the mixture is stirred. With single-channel spectrophotometers, the reaction is monitored at a single wavelength by measuring the absorbance as a function of time. Array-detector-based instruments allow entire spectra to be taken at different time intervals for later analysis.

[23]For the conditions necessary for an enzyme reaction to be in its initial stages, see J. D. Ingle Jr. and S. R. Crouch, *Anal. Chem.*, **1971**, *43*, 697, **DOI**: 10.1021/ac60301a007.

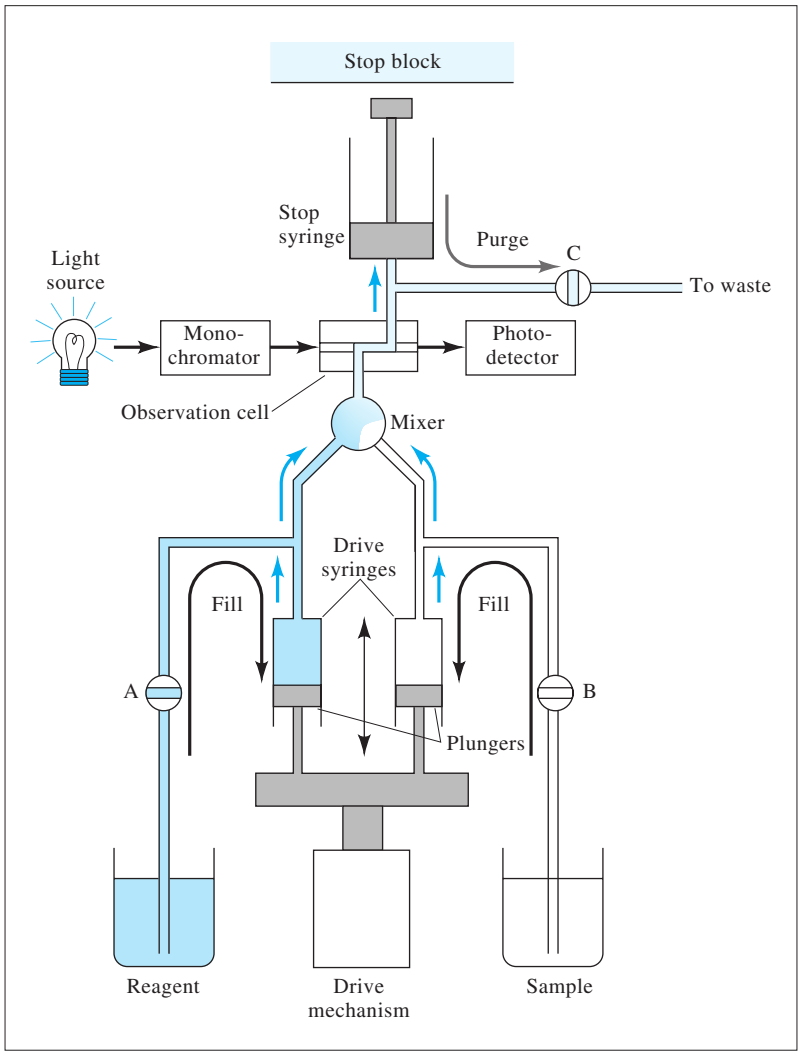

FIGURE 14-16 Stopped-flow mixing apparatus. To begin the experiment, the drive syringes are filled with reagent and sample, and valves A, B, and C are closed. The drive mechanism is then activated to move the drive syringe plungers forward rapidly. The reagent and sample are mixed in the mixer and pass immediately into the observation cell and stop syringe. When the stop syringe fills, the plunger strikes the stop block and the flow ceases almost instantly with a recently mixed plug of solution in the spectrophotometric observation cell. For well-designed systems, the time between mixing and observation can be on the order of 2 to 4 ms.

Continuous flow methods, such as flow injection analysis (see Chapter 33), are also used for sample introduction and reaction monitoring. A popular method with flow injection is to introduce sample and reagents in flowing streams and then to stop the flow with the reaction mixture in the spectrophotometric flow cell. For reactions with half-lives of less than 10 s, the *stopped-flow mixing* technique is popular. In this technique, streams of reagent and sample are mixed rapidly, and the flow of mixed solution is stopped suddenly. The reaction progress is then monitored at a position slightly downstream from the mixing point. The apparatus shown in Figure 14-16 is designed to perform stopped-flow mixing and to allow measurements on the millisecond time scale.

14F-3 Types of Kinetic Methods

Kinetic methods can be classified according to how the measurement is made.[24] *Differential methods* compute the rate of reaction and relate it to the analyte concentration. Rates are determined

[24]For spreadsheet approaches to kinetic methods, see S. R. Crouch and F. J. Holler, *Applications of Microsoft® Excel in Analytical Chemistry*, 3rd ed., Chap. 13, Belmont, CA: Cengage Learning, 2017.

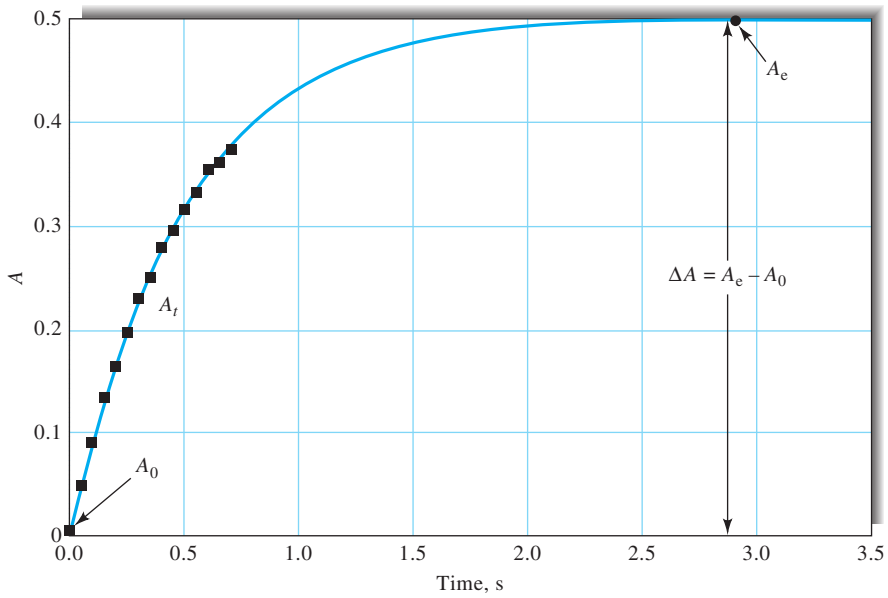

FIGURE 14-17 The predictive approach in kinetic methods. A mathematical model, shown as the solid line, is used to fit the response, shown as the squares, during the kinetic regime of a reaction. The model is then used to predict the equilibrium absorbance, A_e, which is related to the analyte concentration. In the example shown, the absorbance is plotted versus time and the early time data used to predict A_e, the equilibrium value, shown as the circle. (From G. E. Mieling and H. L. Pardue, *Anal. Chem.*, **1978**, *50*, 1611–1618, **DOI**: 10.1021/ac50034a011. American Chemical Society.)

from the slope of the absorbance versus time curve. *Integral methods* use an integrated form of the rate equation and determine the concentration of analyte from the absorbance changes that occur over various time intervals. Curve-fitting methods fit a mathematical model to the absorbance versus time curve and compute the parameters of the model, including the analyte concentration. The most sophisticated of these methods use the parameters of the model to estimate the value of the equilibrium or steady-state response. These methods can provide error compensation because the equilibrium position is less sensitive to such experimental variables as temperature, pH, and reagent concentrations. Figure 14-17 illustrates the use of this approach to predict the equilibrium absorbance from data obtained during the kinetic regime of the absorbance versus time curve. The equilibrium absorbance is then related to the analyte concentration in the usual way.

14G SPECTROPHOTOMETRIC STUDIES OF COMPLEX IONS

Spectrophotometry is a valuable tool for discovering the composition of complex ions in solution and for determining their formation constants (K_f values). Quantitative absorption measurements are very useful for studying complexation because they can be made without disturbing the equilibria under consideration. Although many spectrophotometric studies of complexes involve systems in which a reactant or a product absorbs radiation, nonabsorbing systems can also be investigated successfully. For example, the composition and formation constant for a complex of iron(II) and a nonabsorbing ligand may often be determined by measuring the absorbance decreases that occur when solutions of the absorbing iron(II) complex of 1,10-phenanthroline are mixed with various amounts of the nonabsorbing ligand. The success of this approach depends on the well-known values of the *formation constant* ($K_f = 2 \times 10^{21}$) and the composition of the 1,10-phenanthroline (3:1) complex of iron(II).

The most common techniques used for complex-ion studies are (1) the method of continuous variations, (2) the mole-ratio method, (3) the slope-ratio method, and (4) computer-based curve-fitting methods.

14G-1 The Method of Continuous Variations

In the method of continuous variations, cation and ligand solutions with identical analytical concentrations are mixed in such a way that the total volume and the total number of moles of reactants in each mixture are constant but the mole ratio of

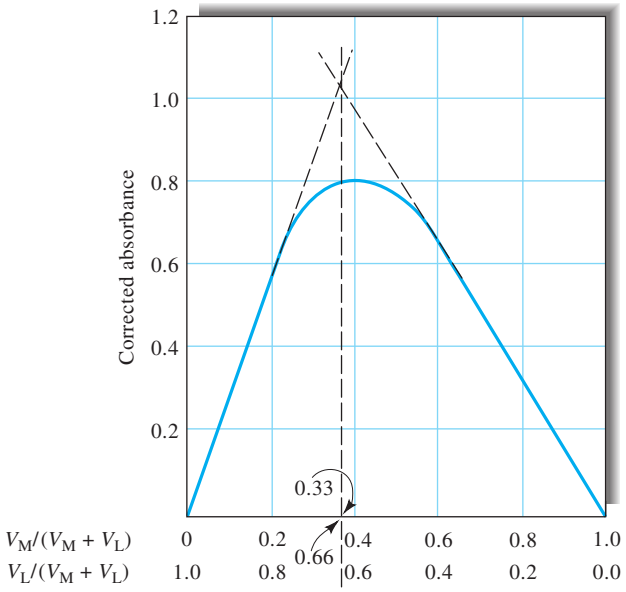

FIGURE 14-18 Continuous-variation plot for the 1:2 complex ML_2.

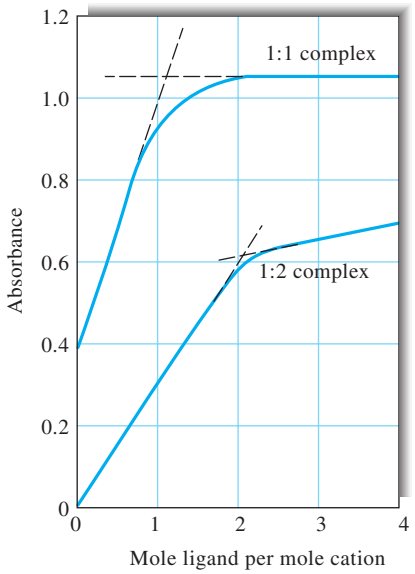

FIGURE 14-19 Mole-ratio plots for a 1:1 and a 1:2 complex. The 1:2 complex is the more stable of the two complexes as indicated by closeness of the experimental curve to the extrapolated lines. The closer the curve is to the extrapolated lines, the larger the formation constant of the complex; the larger the deviation from the straight lines, the smaller the formation constant of the complex.

reactants varies systematically (for example, 9:1, 8:2, 7:3, and so forth). The absorbance of each solution is then measured at a suitable wavelength and corrected for any absorbance the mixture might exhibit if no reaction had occurred. For example, if only the ligand absorbs UV or visible radiation, the corrected absorbance would be the absorbance of the reaction mixture minus the absorbance of the ligand had it not reacted. The corrected absorbance is plotted against the volume fraction of one reactant, that is, $V_M/(V_M + V_L)$, where V_M is the volume of the cation solution and V_L is the volume of the ligand solution. A typical continuous-variations plot is shown in Figure 14-18. A maximum (or minimum if the complex is less absorbing than the reactants) occurs at a volume ratio V_M/V_L corresponding to the combining ratio of cation and ligand in the complex. In Figure 14-18, $V_M/(V_M + V_L)$ is 0.33 and $V_L/(V_M + V_L)$ is 0.66; thus, V_M/V_L is 0.33/0.66, which suggests that the complex has the formula ML_2.[25]

The curvature of the experimental lines in Figure 14-18 is the result of incompleteness of the complex-formation reaction. The formation constant for the complex can be evaluated from measurements of the deviations from the theoretical straight lines, which represent the curve that would result if the reaction between the ligand and the metal proceeded to completion.

[25]A spreadsheet approach for the method of continuous variation is given in S. R. Crouch and F. J. Holler, *Applications of Microsoft® Excel in Analytical Chemistry*, 3rd ed., Chap. 12, Belmont, CA: Cengage Learning, 2017.

Mathematical models can be derived to allow calculation of the K_f value or computer curve-fitting methods can be used (see section 14G-4).

14G-2 The Mole-Ratio Method

In the mole-ratio method, a series of solutions is prepared in which the analytical concentration of one reactant (usually the cation) is held constant while that of the other is varied. A plot of absorbance versus mole ratio of the reactants is then prepared. If the formation constant is reasonably favorable, two straight lines of different slopes that intersect at a mole ratio that corresponds to the combining ratio in the complex are obtained. Typical mole-ratio plots are shown in Figure 14-19. Notice that the ligand of the 1:2 complex absorbs at the wavelength selected so that the slope beyond the equivalence point is greater than zero. We deduce that the uncomplexed cation involved in the 1:1 complex absorbs radiation, because the initial point has an absorbance greater than zero.

Formation constants can be evaluated from the data in the curved portion of mole-ratio plots where the reaction is least complete. If two or more complexes form, successive slope changes in the mole-ratio plot may occur provided the complexes have different molar absorptivities and different formation constants.

14G-3 The Slope-Ratio Method

This approach is particularly useful for weak complexes but is applicable only to systems in which a single complex is formed. The method assumes (1) that the complex-formation reaction can be forced to completion by a large excess of either reactant and (2) that Beer's law is followed under these circumstances.

Let us consider the reaction in which the complex M_xL_y is formed by the reaction of x moles of the cation M with y moles of a ligand L:

$$xM + yL \rightleftharpoons M_xL_y$$

Mass-balance expressions for this system are

$$c_M = [M] + x[M_xL_y]$$

$$c_L = [L] + y[M_xL_y]$$

where c_M and c_L are the molar analytical concentrations of the two reactants. We now assume that at very high analytical concentrations of L, the equilibrium is shifted far to the right and $[M] \ll x[M_xL_y]$. Under this condition, the first mass-balance expression simplifies to

$$c_M = x[M_xL_y]$$

If the system obeys Beer's law,

$$A_1 = \varepsilon b[M_xL_y] = \varepsilon b c_M / x$$

where ε is the molar absorptivity of M_xL_y and b is the path length. A plot of absorbance as a function of c_M is linear when there is sufficient L present to justify the assumption that $[M] \ll x[M_xL_y]$. The slope of this plot is $\varepsilon b/x$.

When c_M is made very large, we assume that $[L] \ll y[M_xL_y]$, and the second mass-balance equation reduces to

$$c_L = y[M_xL_y]$$

and

$$A_2 = \varepsilon b[M_xL_y] = \varepsilon b c_L / y$$

Again, if our assumptions are valid, we find that a plot of A versus c_L is linear at high concentrations of M. The slope of this line is $\varepsilon b/y$.

Simulation: Learn more about **determining the composition of complexes** at www.tinyurl.com/skoogpia7

The ratio of the slopes of the two straight lines gives the combining ratio between M and L:

$$\frac{\varepsilon b/x}{\varepsilon b/y} = \frac{y}{x}$$

14G-4 Computer-Based Methods for Determining Formation Constants of Complexes

Several different methods depend on computer curve fitting to determine formation constants of complexes. We illustrate one approach here, but many others are used.[26]

Principles

Let us consider the formation of a single 1:1 complex ML from metal ion M and ligand L. Once again, we leave the charges off for generality:

$$M + L \rightleftharpoons ML \qquad K_f = \frac{[ML]}{[M][L]}$$

If the uncomplexed metal ion and the complex both absorb radiation at the analysis wavelength, we can write

$$A = \varepsilon_{ML} b[ML] + \varepsilon_M b[M] \tag{14-7}$$

The mass-balance expression for the metal ion is

$$c_M = [M] + [ML]$$

If we solve for [M] and substitute into Equation 14-7, we get

$$A = \varepsilon_{ML} b[ML] + \varepsilon_M b(c_M - [ML])$$

$$= \varepsilon_{ML} b[ML] + \varepsilon_M b c_M - \varepsilon_M b[ML] \tag{14-8}$$

When the ligand concentration is zero, $[ML] = 0$ and the absorbance $A_{L=0}$ is given by

$$A_{L=0} = \varepsilon_M b c_M$$

[26]See for example, K. A. Connors, *Binding Constants: The Measurement of Molecular Complex Stability*, New York: Wiley, 1988; F. J. C. Rossotti and H. Rossotti, *The Determination of Stability Constants*, New York: McGraw-Hill, 1961.

If we substitute this expression into Equation 14-8 and rearrange, we get

$$\Delta A = A - A_{L=0} = \varepsilon_{ML} b[ML] - \varepsilon_M b[ML]$$
$$= \Delta\varepsilon b[ML] \qquad (14\text{-}9)$$

where ΔA is the difference in absorbance with and without the ligand present, and $\Delta\varepsilon$ is the difference in the molar absorptivities of ML and M.

From the formation constant expression, we can write $[ML] = K_f \times [M][L]$. Furthermore, if our experiments are carried out in the presence of excess ligand, $c_L \approx [L]$. Substituting these expressions and the mass balance expression for [M] into Equation 14-9, we obtain

$$\frac{\Delta A}{b} = \Delta\varepsilon K_f c_L[M] = \Delta\varepsilon K_f c_L\{c_M - [ML]\}$$

This expression can be manipulated to obtain

$$\frac{\Delta A}{b} = \frac{\Delta\varepsilon K_f c_L c_M}{1 + K_f c_L} \qquad (14\text{-}10)$$

Data Analysis

Equation 14-10 is the basis for several computer-based methods for determining the formation constant K_f. In the usual experiment, a constant concentration of metal is used and the total ligand concentration c_L is varied. The change in absorbance ΔA is then measured as a function of total ligand concentration and the results statistically analyzed to obtain K_f. Unfortunately, the relationship shown in Equation 14-10 is nonlinear, and thus nonlinear regression must be used unless the equation is transformed to a linear form.[27] We can linearize the equation by taking the reciprocal of both sides to obtain

$$\frac{b}{\Delta A} = \frac{1 + K_f c_L}{\Delta\varepsilon K_f c_L c_M} = \frac{1}{\Delta\varepsilon K_f c_L c_M} + \frac{1}{\Delta\varepsilon c_M} \qquad (14\text{-}11)$$

A double reciprocal plot of $b/\Delta A$ versus $1/c_L$ should be a straight line with a slope of $1/\Delta\varepsilon K_f c_M$ and an intercept of $1/\Delta\varepsilon c_M$. This equation is sometimes called the Benesi-Hildebrand equation.[28]

Linear regression can thus be used to obtain the formation constant as well as $\Delta\varepsilon$ if c_M is known. The least-squares parameters obtained are optimal only for the linearized equation and may not be the optimum values for the nonlinear equation. Hence, nonlinear regression is usually preferred for determining the parameters K_f and $\Delta\varepsilon$. Many computer programs are available for nonlinear regression. Spreadsheet programs such as Excel can be used, but they do not give statistical estimates of the goodness of fit or standard errors for the parameters. Example 14-3 illustrates the use of Excel for these calculations. Other programs, including Origin, Minitab, GraphPad Prism, SigmaPlot, and TableCurve, give more complete statistics.

EXAMPLE 14-3

To obtain the formation constant of a 1:1 complex, the absorbance data in the following table were obtained at various ligand concentrations and a metal concentration of 1.00×10^{-3} M. Both the uncomplexed metal ion and the complex absorb radiation at the analysis wavelength. The cell path length was 10 cm. Use a spreadsheet to determine the formation constant.

[L], M	*A*
0.0500	1.305
0.0400	1.215
0.0300	1.158
0.0200	1.034
0.0100	0.787
0.0050	0.525
0.0000	0.035

Solution

We will first use Equation 14-11, the linearized form of Equation 14-10. Here, we need to calculate $1/[L]$ and $b/\Delta A$. The resulting spreadsheet is shown in Figure 14-20. The value of K_f determined by this method is 96 and $\Delta\varepsilon$ is 152. Next we will use Excel's Solver to obtain the results for the nonlinear Equation 14-10.[29] We start out with initial estimates of the parameters $K_f = 10$ and $\Delta\varepsilon = 50$. As can be seen in Figure 14-21a, the fit is not good with these values. Using the initial estimates we can calculate the values predicted by the model and obtain the differences between the model and the data values (residuals). Solver then minimizes the sum of the squares of the residuals to obtain the best-fit values shown in Figure 14-21b. The fit is now quite good, as seen in the plot. The nonlinear regression parameters are $K_f = 97$ and $\Delta\varepsilon = 151$.

[27] See D. A. Skoog, D. M. West, F. J. Holler, and S. R. Crouch, *Fundamentals of Analytical Chemistry*, 9th ed., Chap. 8, Belmont, CA: Brooks/Cole, 2014.

[28] H. Benesi and J. H. Hildebrand, *J. Am. Chem. Soc.*, **1949**, *71*, 2703, **DOI**: 10.1021/ja01176a030.

[29] For more information on nonlinear regression using Excel, see S. R. Crouch and F. J. Holler, *Applications of Microsoft® Excel in Analytical Chemistry*, 3rd ed., Chap. 13, Belmont, CA: Cengage Learning, 2017.

	A	B	C	D	E	F	G
1	**Double Reciprocal Plot**						
2	b	10.0	cm				
3	c_M	1.00E-03	M				
4	A	[L]	$\Delta A/b$	1/[L]	$b/\Delta A$		
5	1.305	0.0500	0.1270	20.0000	7.874016		
6	1.215	0.0400	0.1180	25.0000	8.474576		
7	1.158	0.0300	0.1123	33.3333	8.90472		
8	1.034	0.0200	0.0999	50.0000	10.01001		
9	0.787	0.0100	0.0752	100.0000	13.29787		
10	0.525	0.0050	0.0490	200.0000	20.40816		
11	0.035	0.0000	0.0000				
12							
13							
14							
15							
16							
17							
18							
19							
20							
21							
22							
23							
24							
25							
26							
27							
28							
29							
30							
31							
32	Intercept	6.585528					
33	Slope	0.068769					
34	K_f	95.76259					
35	$\Delta\varepsilon$	151.85					
36	**Spreadsheet Documentation**						
37	Cell C5=(A5-$A$11)/$B$2						
38	Cell D5=1/B5						
39	Cell E5=1/C5						
40	Cell B32=INTERCEPT(E5:E10,D5:D10)						
41	Cell B33=SLOPE(E5:E10,D5:D10)						
42	Cell B34=B32/B33						
43	Cell B35=1/(B32*B31)						

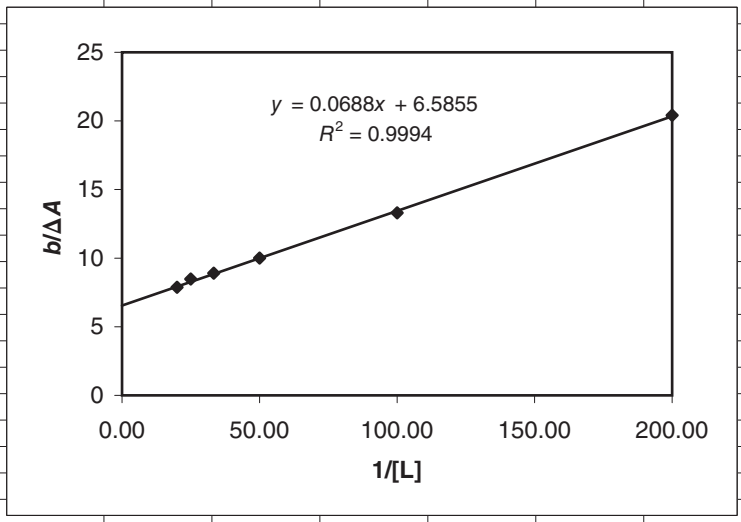

FIGURE 14-20 Spreadsheet to calculate the formation constant of a complex from absorbance data using a double reciprocal plot. Equation 14-10 is linearized by calculating the reciprocals in columns D and E. The least-squares slope and intercept are given in the plot and in the cells below the plot. The parameters K_f and $\Delta\varepsilon$ are calculated in cells B34 and B35.

Extensions to Complicated Equilibria

Equation 14-10 can be modified to fit many other cases. It can be extended to account for the formation of polynuclear complexes and for multiple equilibria. UV and visible absorption spectroscopy is not, however, particularly well suited for multiple equilibria because of its lack of specificity and because each additional equilibrium adds two unknowns, a formation constant term and a molar absorptivity term.

The introduction of array-detector spectrometric systems has brought about several new data analysis approaches. Instead of using data at only a single wavelength, these approaches can simultaneously use data at multiple wavelengths. With modern computers, equations similar to Equation 14-10 can be fit nearly simultaneously at multiple wavelengths using curve-fitting programs such as TableCurve (Systat Software).

	A	B	C	D	E	F	G
1	**Nonlinear Regression**						
2	b	10.0	cm				
3	c_M	1.00E-03	M				
4	A	[L]	$\Delta A/b$	Model	Residuals	Squares	
5	1.305	0.0500	0.1270	0.016667	0.1103	0.012173	
6	1.215	0.0400	0.1180	0.014286	0.1037	0.010757	
7	1.158	0.0300	0.1123	0.011538	0.1008	0.010153	
8	1.034	0.0200	0.0999	0.008333	0.0916	0.008384	
9	0.787	0.0100	0.0752	0.004545	0.0707	0.004992	
10	0.525	0.0050	0.0490	0.002381	0.0466	0.002173	
11	0.035	0.0000	0.0000	0	0.0000	0	
12					SSR	0.048633	
13–33	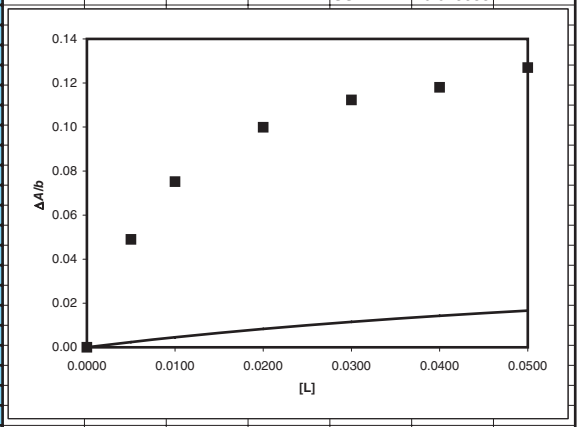						
34	K_f	10					
35	$\Delta\varepsilon$	50					
36	**Spreadsheet Documentation**						
37	Cell C5=(A5-$A$11)/$B$2						
38	Cell D5=$B$34*B$35*$B$3*B5/(1+$B$34*B5)						
39	Cell E5=C5-D5						
40	Cell F5=E5^2						
41	Cell F12=SUM(F5:F10)						
42	Cell B34=Initial estimate or Solver result						
43	Cell B35=Initial estimate or Solver result						

(a)

	A	B	C	D	E	F	G
1	**Nonlinear Regression**						
2	b	10.0	cm				
3	c_M	1.00E-03	M				
4	A	[L]	$\Delta A/b$	Model	Residuals	Squares	
5	1.305	0.0500	0.1270	0.125225	0.0018	3.15E-06	
6	1.215	0.0400	0.1180	0.12011	-0.0021	4.45E-06	
7	1.158	0.0300	0.1123	0.112454	-0.0002	2.37E-08	
8	1.034	0.0200	0.0999	0.099739	0.0002	2.59E-08	
9	0.787	0.0100	0.0752	0.074476	0.0007	5.24E-07	
10	0.525	0.0050	0.0490	0.049434	-0.0004	1.89E-07	
11	0.035	0.0000	0.0000	0	0.0000	0	
12					SSR	8.36E-06	
13–33	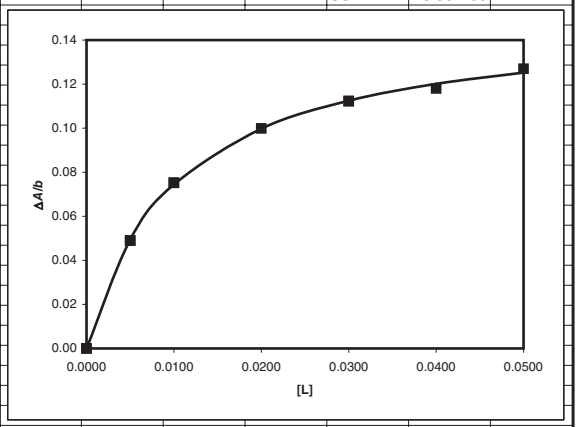						
34	K_f	97.40448					
35	$\Delta\varepsilon$	150.9375					
36	**Spreadsheet Documentation**						
37	Cell C5=(A5-$A$11)/$B$2						
38	Cell D5=$B$34*B$35*$B$3*B5/(1+$B$34*B5)						
39	Cell E5=C5-D5						
40	Cell F5=E5^2						
41	Cell F12=SUM(F5:F10)						
42	Cell B34=Initial estimate or Solver result						
43	Cell B35=Initial estimate or Solver result						

(b)

FIGURE 14-21 Spreadsheets to calculate formation constants using nonlinear regression. (a) The results from the model (Equation 14-10) are calculated in column D using the initial estimates of $K_f = 10$ and $\Delta\varepsilon = 50$. The plot shows the model values (solid line) and the data values (points). The difference between the data values (column C) and the model values (column D) are the residuals shown in column E. The squares of these are calculated in column F and summed in cell F12 (SSR). In (b), Excel's Solver has minimized the value in cell F12 to obtain the best-fit values shown in cells B34 and B35. The model values are again shown as the solid line in the plot.

If formation constants are known or determined by the above methods, several programs are available for determining the species composition at various concentrations. The programs HALTAFALL[30] and COMICS[31] have been popular for many years for speciation in complex systems. These programs use the formation constants and mass-balance expressions to calculate the species composition as a function of initial concentrations. Several modern versions, including some that operate in the Windows environment, are available.

[30]N. Ingri, W. Kalolowicz, L. G. Sillén, and B. Warnqvist, *Talanta*, **1967**, *14*, 1261, **DOI**: 10.1016/0039-9140(67)80203-0.

[31]D. D. Perrin and I. G. Sayce, *Talanta*, **1967**, *14*, 833, **DOI**: 10.1016/0039-9140(67)80105-X.

» QUESTIONS AND PROBLEMS

*Answers are provided at the end of the book for problems marked with an asterisk.

Problems with this icon are best solved using spreadsheets.

***14-1** A 25.0-mL aliquot of an aqueous quinine solution was diluted to 50.0 mL and found to have an absorbance of 0.636 at 348 nm when measured in a 2.50-cm cell. A second 25.0-mL aliquot was mixed with 10.00 mL of a solution containing 23.1 ppm of quinine; after dilution to 50.0 mL, this solution had an absorbance of 0.903 (2.50-cm cell). Calculate the concentration of quinine in parts per million in the sample.

***14-2** A 0.4740-g pesticide sample was decomposed by wet ashing and then diluted to 200.0 mL in a volumetric flask. The analysis was completed by treating aliquots of this solution as indicated.

Volume of Sample Taken, mL	Reagent Volumes Used, mL			Absorbance, *A*, 545 nm (1.00-cm cells)
	2.50 ppm Cu^{2+}	Ligand	H_2O	
5.00	0.00	20.0	25.0	0.671
5.00	1.00	20.0	24.0	0.849

Calculate the percentage of copper in the sample.

14-3 Sketch a photometric titration curve for the titration of Sn^{2+} with MnO_4^-. What color radiation should be used for this titration? Explain.

14-4 Iron(III) reacts with thiocyanate ion to form the red complex $Fe(SCN)^{2+}$. Sketch a photometric titration curve for Fe(III) with thiocyanate ion when a photometer with a green filter is used to collect data. Why is a green filter used?

14-5 EDTA abstracts bismuth(III) from its thiourea complex:

$$Bi(tu)_6^{3+} + H_2Y^{2-} \rightarrow BiY^- + 6tu + 2H^+$$

where tu is the thiourea molecule $(NH_2)_2CS$. Predict the shape of a photometric titration curve based on this process, given that the Bi(III) or thiourea complex is the only species in the system that absorbs light at 465 nm, the wavelength selected for the analysis.

***14-6** The accompanying data (1.00-cm cells) were obtained for the spectrophotometric titration of 10.00 mL of Pd(II) with 2.44×10^{-4} M Nitroso R (O. W. Rollins and M. M. Oldham, *Anal. Chem.*, **1971**, *43*, 262, **DOI**: 10.1021/ac60297a026).

Volume of Nitroso R, mL	A_{500}
0	0
1.00	0.147
2.00	0.271
3.00	0.375

Calculate the concentration of the Pd(II) solution, given that the ligand-to-cation ratio in the colored product is 2:1

***14-7** A 3.03-g petroleum specimen was decomposed by wet ashing and subsequently diluted to 500 mL in a volumetric flask. Cobalt was determined by treating 25.00-mL aliquots of this diluted solution as follows:

Reagent Volume, mL			
Co(II), 4.00 ppm	Ligand	H_2O	Absorbance (1.00-cm cell)
0.00	20.00	5.00	0.212
5.00	20.00	0.00	0.399

QUESTIONS AND PROBLEMS (continued)

Assume that the Co(II)-ligand chelate obeys Beer's law, and calculate the percentage of cobalt in the original sample.

***14-8** A simultaneous determination for cobalt and nickel can be based on absorption by their respective 8-hydroxyquinolinol complexes. Molar absorptivities corresponding to their absorption maxima are as follows:

	Molar Absorptivity, ε	
	365 nm	**700 nm**
Co	3529	428.9
Ni	3228	10.2

Calculate the molar concentration of nickel and cobalt in each of the following solutions using the following data:

	Absorbance, *A* (1.00-cm cells)	
Solution	**365 nm**	**700 nm**
(a)	0.349	0.022
(b)	0.792	0.081

***14-9** When measured with a 1.00-cm cell, a 7.50×10^{-5} M solution of species A exhibited absorbances of 0.155 and 0.755 at 475 and 700 nm, respectively. A 4.25×10^{-5} M solution of species B gave absorbances of 0.702 and 0.091 under the same circumstances. Calculate the concentrations of A and B in solutions that yielded the following absorbance data in a 2.50-cm cell: (a) 0.439 at 475 nm and 1.025 at 700 nm; (b) 0.662 at 475 nm and 0.815 at 700 nm.

***14-10** The acid-base indicator HIn undergoes the following reaction in dilute aqueous solution:

$$\underset{\text{color 1}}{\text{HIn}} \rightleftharpoons \text{H}^+ + \underset{\text{color 2}}{\text{In}^-}$$

The following absorbance data were obtained for a 5.00×10^{-4} M solution of HIn in 0.1 M NaOH and 0.1 M HCl. Measurements were made at wavelengths of 485 nm and 625 nm with 1.00-cm cells.

$$\text{0.1 M NaOH} \quad A_{485} = 0.075 \quad A_{625} = 0.904$$

$$\text{0.1 M HCl} \quad A_{485} = 0.487 \quad A_{625} = 0.181$$

In the NaOH solution, essentially all of the indicator is present as In^-; in the acidic solution, it is essentially all in the form of HIn.

(a) Calculate molar absorptivities for In^- and HIn at 485 and 625 nm.

(b) Calculate the acid dissociation constant for the indicator if a pH 5.00 buffer containing a small amount of the indicator exhibits an absorbance of 0.567 at 485 nm and 0.395 at 625 nm (1.00-cm cells).

(c) What is the pH of a solution containing a small amount of the indicator that exhibits an absorbance of 0.492 at 485 nm and 0.245 at 635 nm (1.00-cm cells)?

(d) A 25.00-mL aliquot of a solution of purified weak organic acid HX required exactly 24.20 mL of a standard solution of a strong base to reach a phenolphthalein end point. When exactly 12.10 mL of the base was added to a second 25.00-mL aliquot of the acid, which contained a small amount of the indicator under consideration, the absorbance was found to be 0.333 at 485 nm and 0.655 at 625 nm (1.00-cm cells). Calculate the pH of the solution and K_a for the weak acid.

(e) What would be the absorbance of a solution at 485 and 625 nm (1.50-cm cells) that was 2.00×10^{-4} M in the indicator and was buffered to a pH of 6.000?

14-11 A standard solution was put through appropriate dilutions to give the concentrations of iron shown next. The iron(II)-1,10,phenanthroline complex was then formed in 25.0-mL aliquots of these solutions, following which each was diluted to 50.0 mL. The following absorbances (1.00-cm cells) were recorded at 510 nm:

Fe(II) Concentration in Original Solutions, ppm	A_{510}
4.00	0.160
10.0	0.390
16.0	0.630
24.0	0.950
32.0	1.260
40.0	l.580

(a) Plot a calibration curve from these data.

(b) Use the method of least squares to find an equation relating absorbance and the concentration of iron(II).

(c) Calculate the standard deviation of the slope and intercept.

14-12 The method developed in Problem 14-11 was used for the routine determination of iron in 25.0-mL aliquots of groundwater. Express the concentration (as ppm Fe) in samples that yielded the accompanying absorbance data (1.00-cm cell). Calculate the relative standard deviation of the result. Repeat the calculation assuming the absorbance data are means of three measurements.

(a) 0.143 **(c)** 0.068 **(e)** 1.512

(b) 0.675 **(d)** 1.009 **(f)** 0.546

14-13 Copper(II) forms a 1:1 complex with the organic complexing agent R in acidic medium. The formation of the complex can be monitored by spectrophotometry at 480 nm. Use the following data collected under pseudo-first-order conditions to construct a calibration curve of rate versus concentration of R. Find the concentration of copper(II) in an unknown whose rate under the same conditions was $6.2 \times 10^{-3} A\ s^{-1}$.

$c_{Cu^{2+}}$, ppm	Rate, $A\ s^{-1}$
3.0	3.6×10^{-3}
5.0	5.4×10^{-3}
7.0	7.9×10^{-3}
9.0	1.03×10^{-2}

* **14-14** Aluminum forms a 1:1 complex with 2-hydroxy-1-naphthaldehyde *p*-methoxybenzoylhydraxonal, which absorbs UV radiation at 285 nm. Under pseudo-first-order conditions, a plot of the initial rate of the reaction (absorbance units per second) versus the concentration of aluminum (in μM) yields a straight line described by the equation

$$\text{rate} = 1.92c_{Al} - 0.250$$

Find the concentration of aluminum in a solution that exhibits a rate of 0.53 absorbance units per second under the same experimental conditions.

QUESTIONS AND PROBLEMS (continued)

*14-15 The enzyme monoamine oxidase catalyzes the oxidation of amines to aldehydes. For tryptamine, K_m for the enzyme is 4.0×10^{-4} M and $v_{max} = k_2[E]_0 = 1.6 \times 10^{-3}$ μM/ min at pH 8. Find the concentration of a solution of tryptamine that reacts at a rate of 0.12 μM/min in the presence of monoamine oxidase under the above conditions. Assume that [tryptamine] $\ll K_m$.

14-16 The sodium salt of 2-quinizarinsulfonic acid (NaQ) forms a complex with Al^{3+} that absorbs radiation strongly at 560 nm.[32] (a) Use the data from Owens and Yoe's paper to find the formula of the complex. In all solutions, $c_{Al} = 3.7 \times 10^{-5}$ M, and all measurements were made in 1.00-cm cells. (b) Find the molar absorptivity of the complex.

c_Q, M	A_{560}
1.00×10^{-5}	0.131
2.00×10^{-5}	0.265
3.00×10^{-5}	0.396
4.00×10^{-5}	0.468
5.00×10^{-5}	0.487
6.00×10^{-5}	0.498
8.00×10^{-5}	0.499
1.00×10^{-4}	0.500

14-17 The accompanying data were obtained in a slope-ratio investigation of the complex formed between Ni^{2+} and 1-cyclopentene-1-dithiocarboxylic acid (CDA). The measurements were made at 530 nm in 1.00-cm cells.

$c_{CDA} = 1.00 \times 10^{-3}$ M		$c_{Ni} = 1.00 \times 10^{-3}$ M	
c_{Ni}, M	A_{530}	c_{CDA}, M	A_{530}
5.00×10^{-6}	0.051	9.00×10^{-6}	0.031
1.20×10^{-5}	0.123	1.50×10^{-5}	0.051
3.50×10^{-5}	0.359	2.70×10^{-5}	0.092
5.00×10^{-5}	0.514	4.00×10^{-5}	0.137
6.00×10^{-5}	0.616	6.00×10^{-5}	0.205
7.00×10^{-5}	0.719	7.00×10^{-5}	0.240

(a) Determine the formula of the complex. Use linear least-squares to analyze the data.

(b) Find the molar absorptivity of the complex and its uncertainty.

[32] E. G. Owens and J. H. Yoe, *Anal. Chem.*, **1959**, *31*, 384, **DOI**: 10.1021/ac60147a016.

14-18 The accompanying absorption data were recorded at 390 nm in 1.00-cm cells for a continuous-variation study of the colored product formed between Cd^{2+} and the complexing reagent R.

	Reagent Volumes, mL		
Solution	$c_{Cd} = 1.25 \times 10^{-4}$ M	$c_R = 1.25 \times 10^{-4}$ M	A_{390}
0	10.00	0.00	0.000
1	9.00	1.00	0.174
2	8.00	2.00	0.353
3	7.00	3.00	0.530
4	6.00	4.00	0.672
5	5.00	5.00	0.723
6	4.00	6.00	0.673
7	3.00	7.00	0.537
8	2.00	8.00	0.358
9	1.00	9.00	0.180
10	0.00	10.00	0.000

(a) Find the ligand-to-metal ratio in the product.

(b) Calculate an average value for the molar absorptivity of the complex and its uncertainty. Assume that in the linear portions of the plot the metal is completely complexed.

(c) Calculate K_f for the complex using the stoichiometric ratio determined in (a) and the absorption data at the point of intersection of the two extrapolated lines.

14-19 Palladium(II) forms an intensely colored complex at pH 3.5 with arsenazo III at 660 nm.[33] A meteorite was pulverized in a ball mill, and the resulting powder was digested with various strong mineral acids. The resulting solution was evaporated to dryness, dissolved in dilute hydrochloric acid, and separated from interferents by ion-exchange chromatography. The resulting solution containing an unknown amount of Pd(II) was then diluted to 50.00 mL with pH 3.5 buffer. Ten-milliliter aliquots of this analyte solution were then transferred to six 50-mL volumetric flasks. A standard solution was then prepared that was 1.00×10^{-5} M in Pd(II). Volumes of the standard solution shown in the table were then pipetted into the volumetric flasks along with 10.00 mL of 0.01 M arsenazo III. Each solution was then diluted to 50.00 mL, and the absorbance of each solution was measured at 660 nm in 1.00-cm cells.

Volume Standard Solution, mL	A_{660}
0.00	0.216
5.00	0.338
10.00	0.471
15.00	0.596
20.00	0.764
25.00	0.850

(a) Enter the data into a spreadsheet, and construct a standard-additions plot of the data.

(b) Determine the slope and intercept of the line.

[33] J. G. Sen Gupta, *Anal. Chem.*, **1967**, *39*, 18, **DOI**: 10.1021/ac60245a029.

QUESTIONS AND PROBLEMS (continued)

(c) Determine the standard deviation of the slope and of the intercept.

(d) Calculate the concentration of Pd(II) in the analyte solution.

(e) Find the standard deviation of the measured concentration.

14-20 Given the information that

$$Fe^{3+} + Y^{4-} \rightleftharpoons FeY^{-} \qquad K_f = 1.0 \times 10^{25}$$

$$Cu^{2+} + Y^{4-} \rightleftharpoons CuY^{2-} \qquad K_f = 6.3 \times 10^{18}$$

and the further information that, among the several reactants and products, only CuY^{2-} absorbs radiation at 750 nm, describe how Cu(II) could be used as an indicator for the photometric titration of Fe(III) with H_2Y^{2-}. Reaction: $Fe^{3+} + H_2Y^{2-} \rightarrow FeY^{-} + 2H^{+}$.

* **14-21** The chelate CuA_2^{2-} exhibits maximum absorption at 480 nm. When the chelating reagent is present in at least a tenfold excess, the absorbance depends only on the analytical concentration of Cu(II) and conforms to Beer's law over a wide range. A solution in which the analytical concentration of Cu^{2+} is 2.15×10^{-4} M and that for A^{2-} is 9.00×10^{-3} M has an absorbance of 0.759 when measured in a 1.00-cm cell at 480 nm. A solution in which the analytical concentrations of Cu^{2+} and A^{2-} are 2.15×10^{-4} M and 4.00×10^{-4} M, respectively, has an absorbance of 0.654 when measured under the same conditions. Use this information to calculate the formation constant K_f for the process

$$Cu^{2+} + 2A^{2-} \rightleftharpoons CuA_2^{2-}$$

* **14-22** Mixing the chelating reagent B with Ni(II) forms the highly colored NiB_2^{2+}, whose solutions obey Beer's law at 395 nm over a wide range. Provided the analytical concentration of the chelating reagent exceeds that of Ni(II) by a factor of 5 (or more), the cation exists, within the limits of observation, entirely in the form of the complex. Use the accompanying data to evaluate the formation constant K_f for the process

$$Ni^{2+} + 2B \rightleftharpoons NiB_2^{2+}$$

Analytical Concentration, M		
Ni^{2+}	B	A_{395} (1.00-cm cells)
2.00×10^{-4}	2.20×10^{-1}	0.718
2.00×10^{-4}	1.50×10^{-3}	0.276

14-23 To determine the formation constant of a 1:1 complex, the following absorbances were measured at 470 nm in a 2.50-cm cell for the ligand concentrations shown. The total metal concentration was $c_M = 7.50 \times 10^{-4}$ M.

[L], M	*A*
0.0750	0.679
0.0500	0.664
0.0300	0.635
0.0200	0.603
0.0100	0.524
0.0050	0.421
0.0000	0.056

(a) Use linear regression and the Benesi-Hildebrand equation (Equation 14-11) to determine the formation constant and the difference in molar absorptivities at 470 nm.

(b) Use nonlinear regression and Equation 14-10 to find the values of K_f and $\Delta\varepsilon$. Start with initial estimates of $K_f = 50$ and $\Delta\varepsilon = 50$.

Challenge Problem

14-24 (a) Prove mathematically that the peak in a continuous-variations plot occurs at a combining ratio that gives the complex composition.

(b) Show that the overall formation constant for the complex ML_n is

$$K_f = \frac{\left(\frac{A}{A_{extr}}\right)c}{\left[c_M - \left(\frac{A}{A_{extr}}\right)c\right]\left[c_L - n\left(\frac{A}{A_{extr}}\right)c\right]^n}$$

where A is the experimental absorbance at a given value on the x-axis in a continuous-variations plot, A_{extr} is the absorbance determined from the extrapolated lines corresponding to the same point on the x-axis, c_M is the molar analytical concentration of the metal, c_L is the molar analytical concentration of the ligand, and n is the ligand-to-metal ratio in the complex.[34]

(c) Under what assumptions is the equation valid?

(d) What is c?

(e) Discuss the implications of the occurrence of the maximum in a continuous-variations plot at a value of less than 0.5.

(f) Calabrese and Khan[35] characterized the complex formed between I_2 and I^- using the method of continuous variations. They combined 2.60×10^{-4} M solutions of I_2 and I^- in the usual way to obtain the following data set. Use the data to find the composition of the I_2/I^- complex.

$V(I_2$ soln), mL	A_{350}
0.00	0.002
1.00	0.121
2.00	0.214
3.00	0.279
4.00	0.312
5.00	0.325
6.00	0.301
7.00	0.258
8.00	0.188
9.00	0.100
10.00	0.001

[34] J. Inczédy, *Analytical Applications of Complex Equilibria*, New York: Wiley, 1976.

[35] V. T. Calabrese and A. Khan, *J. Phys. Chem. A*, **2000**, *104*, 1287, **DOI**: 10.1021/jp992847r.

QUESTIONS AND PROBLEMS (continued)

(g) The continuous-variations plot appears to be asymmetrical. Consult the paper by Calabrese and Khan and explain this asymmetry.

(h) Use the equation in part (a) to determine the formation constant of the complex for each of the three central points on the continuous-variations plot.

(i) Explain any trend in the three values of the formation constant in terms of the asymmetry of the plot.

(j) Find the uncertainty in the formation constant determined by this method.

(k) What effect, if any, does the formation constant have on the ability to determine the composition of the complex using the method of continuous variations?

(l) Discuss the various advantages and potential pitfalls of using the method of continuous variations as a general method for determining the composition and formation constant of a complex compound.